Stem Cell Reports
Article

OPEN ACCESS

Efficient Ex Vivo Engineering and Expansion of Highly Purified Human Hematopoietic Stem and Progenitor Cell Populations for Gene Therapy

Erika Zonari,[1] Giacomo Desantis,[1] Carolina Petrillo,[1,2] Francesco E. Boccalatte,[1] Maria Rosa Lidonnici,[1] Anna Kajaste-Rudnitski,[1] Alessandro Aiuti,[1,2,3] Giuliana Ferrari,[1,2] Luigi Naldini,[1,2] and Bernhard Gentner[1,4,*]
[1]San Raffaele Telethon Institute for Gene Therapy (SR-TIGET), Milan 20132, Italy
[2]Vita-Salute San Raffaele University, Milan 20132, Italy
[3]Pediatric Immunohematology and Bone Marrow Transplantation Unit, IRCSS Ospedale San Raffaele, Milan 20132, Italy
[4]Hematology and Bone Marrow Transplantation Unit
IRCSS Ospedale San Raffaele, Milan 20132, Italy
*Correspondence: gentner.bernhard@hsr.it
http://dx.doi.org/10.1016/j.stemcr.2017.02.010

SUMMARY

Ex vivo gene therapy based on CD34$^+$ hematopoietic stem cells (HSCs) has shown promising results in clinical trials, but genetic engineering to high levels and in large scale remains challenging. We devised a sorting strategy that captures more than 90% of HSC activity in less than 10% of mobilized peripheral blood (mPB) CD34$^+$ cells, and modeled a transplantation protocol based on highly purified, genetically engineered HSCs co-infused with uncultured progenitor cells. Prostaglandin E_2 stimulation allowed near-complete transduction of HSCs with lentiviral vectors during a culture time of less than 38 hr, mitigating the negative impact of standard culture on progenitor cell function. Exploiting the pyrimidoindole derivative UM171, we show that transduced mPB CD34$^+$CD38$^-$ cells with repopulating potential could be expanded ex vivo. Implementing these findings in clinical gene therapy protocols will improve the efficacy, safety, and sustainability of gene therapy and generate new opportunities in the field of gene editing.

INTRODUCTION

Introduction of the lentiviral vector (LV) platform has spurred applications of gene therapy based on the transplantation of ex-vivo-engineered, autologous hematopoietic stem and progenitor cells (HSPCs) (Naldini, 2015). Recent clinical trials for patients affected by primary immunodeficiencies, hemoglobinopathies, or inborn errors of metabolism have shown high levels of gene transfer into HSPCs, which were stably maintained in multiple hematopoietic lineages until the latest follow-up, reaching up to 9 years in the earliest trial (Cartier et al., 2009; Aiuti et al., 2013; Biffi et al., 2013; Hacein-Bey Abina et al., 2015; Sessa et al., 2016). The post-transplant hematopoiesis reconstituted by polyclonal, gene-marked HSPCs has provided substantial and sustained therapeutic benefit to most treated patients to date. Contrary to the gene therapy trials performed with gamma-retroviral vectors, no adverse events related to insertional mutagenesis of semi-randomly integrating LVs have been reported to date, even though substantial integration loads, typically ranging over 5–20 million integrations per kg body weight, have now been infused into >150 patients. The side effects reported in these gene therapy trials are typically related to the conditioning regimen and include mucositis and temporary bone marrow (BM) aplasia. Trials employing full myeloablation and BM-derived transduced CD34$^+$ cells often showed more prolonged grade 4 neutropenia and thrombocytopenia than allogeneic BM transplantation, despite administering at least similar doses of CD34$^+$ cells/kg (Sessa et al., 2016). Delayed recovery may be caused by the ex vivo culture of the cell therapy product, which typically lasts more than 60 hr (Aiuti et al., 2013; Biffi et al., 2013). Indeed, experimental evidence has accumulated that cultured HSPCs progressively lose engraftment potential by recruitment into cell cycle and loss of adhesion molecules, thus impeding their homing into the niche and driving lineage commitment and differentiation (Glimm et al., 2000; Kallinikou et al., 2012; Larochelle et al., 2012). This notion contrasts with recent reports on successful ex vivo cord blood (CB) expansion leading to accelerated hematologic recovery in patients (reviewed in Kiernan et al., 2016). Differences among HSPC sources (CB versus BM or mobilized peripheral blood [mPB]) may contribute to diverging outcomes, and a complete understanding is key to harnessing emerging CB expansion protocols for ex vivo gene transfer procedures, which utilize BM or mPB HSPCs. Moreover, CD34$^+$ HSPCs comprise a heterogeneous mixture of progenitors at various stages of lineage commitment, the composition of which changes according to age, cell source, and mobilization procedure, and studies investigating the impact of ex vivo culture on defined subpopulations are lacking. Only a minute fraction of these CD34$^+$ cells corresponds to long-term (LT) hematopoietic stem cells (HSCs). Limiting-dilution transplants into immunodeficient mice indicate that no more than 0.1% of lineage-negative CB cells (50%–75% CD34$^+$) engraft longterm (McDermott et al., 2010). In line with an even lower HSC frequency in BM or mPB CD34$^+$ cells, capture/re-capture statistics performed on longitudinally sampled LV integration sites

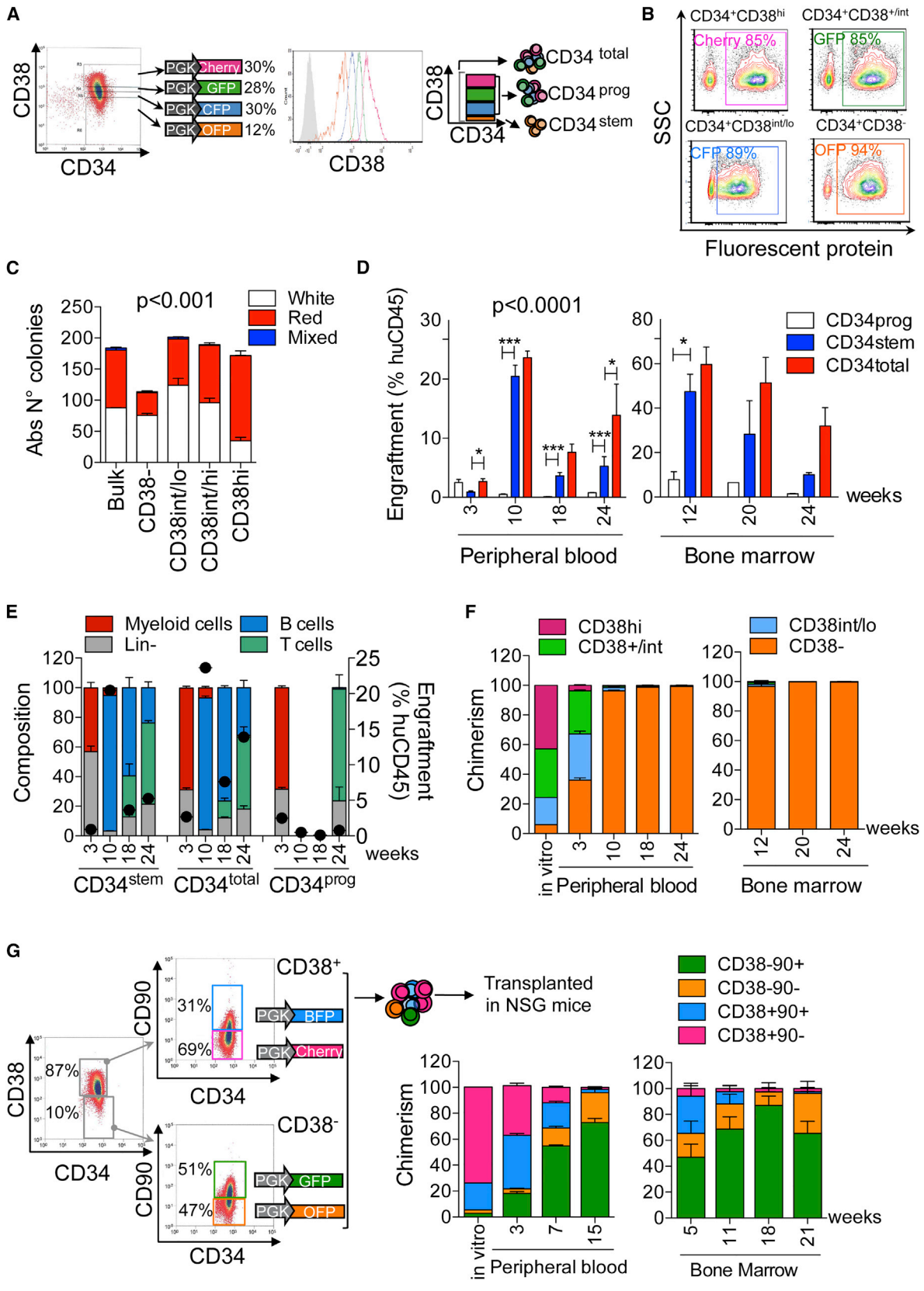

(legend on next page)

from patients treated by gene therapy indicate that ~0.01% of the infused CD34$^+$ cells contribute to long-term hematopoiesis (Aiuti et al., 2013; Biffi et al., 2013; Biasco et al., 2015). These data indicate that there is a substantial margin to more precisely tailor gene transfer to LT-HSCs as opposed to the bulk of CD34$^+$ cells, adapting ex vivo manipulation specifically to the requirements of the therapeutically relevant cell subsets. Several landmark studies have identified surface markers that allow prospective isolation of functionally diverse HSPC subsets (Majeti et al., 2007; Notta et al., 2011). However, most of these studies were done on CB cells that did not undergo ex vivo culture, making the results not necessarily representative of the cells typically used in HSPC gene therapy trials. Furthermore, most studies functionally validating HSC markers employed binary sorting gates (marker^{positive} versus marker^{negative}). Given that antibody staining for many HSPC markers, such as CD38, CD49f, and CD90, results in a gradient of cells with increasing antigen density rather than clearly segregating two populations, large proportions of HSPCs with an intermediate phenotype have not been analyzed in these functional assays.

Here we undertake a comprehensive strategy to advance ex vivo genetic engineering of HSPCs for gene therapy. We experimentally define an optimal, clinically applicable strategy to purify HSCs, which allows uncoupling long-term from short-term hematopoietic reconstitution, and implement ex vivo conditions that best preserve their biological properties applying transduction-enhancing compounds and pyrimidoindole derivatives to support ex vivo HSC expansion.

RESULTS

Definition of Functionally Distinct CD34$^+$ Subpopulations in the Setting of Ex Vivo Gene Therapy

We devised an experimental model that allows tracing the origin of human hematopoiesis to diverse CD34$^+$ HSPC subpopulations, defined at transplantation, in a xenograft over 6 months. First, we sorted CD34$^+$ cells from mPB into four subpopulations according to CD38 expression and stably marked each with a different LV expressing one of the following fluorescent proteins (FP): green FP (GFP), red FP (Cherry), cyan/blue FP (CFP/BFP), or orange FP (OFP) (Figures 1A and S1A). By setting closely spaced sorting gates encompassing the CD38^{dim} populations, we could interrogate the entire CD34$^+$ cell population for differential engraftment potential. In vitro assays confirmed similarly high (>85%) transduction efficiencies for all subpopulations (Figures 1B and S1B) and reduced, myeloid-biased colony-forming capacity within the most primitive CD34$^+$CD38$^-$ fraction (Figures 1C and S1C). One day after transduction, we re-assembled the following cell populations for xenotransplantation: CD34^{total} (all four subpopulations re-assembled to the original proportions at sorting), CD34^{prog} (the three CD38$^+$ subpopulations), and CD34^{stem} (the subpopulation with the 10% lowest CD38 expression). CD34^{stem} cells showed little engraftment at 3 weeks but neared the level of the CD34^{total} group 2 months post-transplantation (Figures 1D and S1D). Instead, CD34^{prog} cells were responsible for the majority of short-term engraftment at 3 weeks post-transplant; their myeloid

Figure 1. In Vivo Tracking of Hematopoietic Reconstitution by CD34$^+$ mPB Subpopulations

(A) Four mPB CD34$^+$ cell subpopulations differing in CD38 expression levels were sorted and transduced with LVs expressing the indicated FPs (PGK, phosphoglycerate kinase promoter). Subpopulation frequency within total CD34$^+$ cells and CD38 expression upon post-sorting re-analysis are shown (histogram plot). The scheme on the right shows how transduced subpopulations were mixed in the three xenotransplantation groups, maintaining their relative frequency at sorting.

(B) Representative transduction efficiency of the indicated subpopulations, as measured in the myeloid colonies after 14 days of culture.

(C) Clonogenic potential of the transduced subpopulations (n = 4 per group). Statistics by one-way ANOVA with Bonferroni's multiple comparison test: white colonies, CD38$^-$ versus CD38$^{int/lo}$ **, CD38$^-$ versus CD38^{hi} *; for red colonies, CD38$^-$ versus Bulk ***, CD38$^-$ versus CD38$^{int/lo}$ **, CD38$^-$ versus CD38$^{int/hi}$ ***, CD38$^-$ versus CD38^{hi} ***.

(D) Human CD45$^+$ cell engraftment in PB and BM at the indicated number of weeks post-transplant (n = 4 mice per group). Data were analyzed by two-way ANOVA with Bonferroni's multiple comparison test, significant differences with respect to the CD34^{stem} group are shown.

(E) Lineage composition (left axis) of the human CD45$^+$ cell graft in the PB at the indicated number of weeks post-transplantation. Black dots indicate huCD45$^+$ cell engraftment levels (right axis). B cells, CD19$^+$; myeloid cells, CD13$^+$, T cells, CD3$^+$; Lin$^-$, CD19$^-$, CD13$^-$, CD3$^-$ cells.

(F) Distribution of the four FPs in the CD34^{total} group before injection (in vitro) or within human CD45$^+$ cells sampled from the PB and BM at the indicated number of weeks post-transplantation allows back-tracking the origin of hematopoietic reconstitution to the originally transplanted cell subpopulations indicated in the legend.

(G) Four subpopulations differing in CD38 and CD90 expression levels were sorted, transduced with the indicated LVs, mixed back maintaining their relative frequency, and xenografted (n = 9 mice, representative experiment). Hematologic reconstitution at the indicated number of weeks post-transplantation in PB and BM is back-tracked to the population of origin, as in (F).

Error bars represent SEM. See also Figures S1–S3.

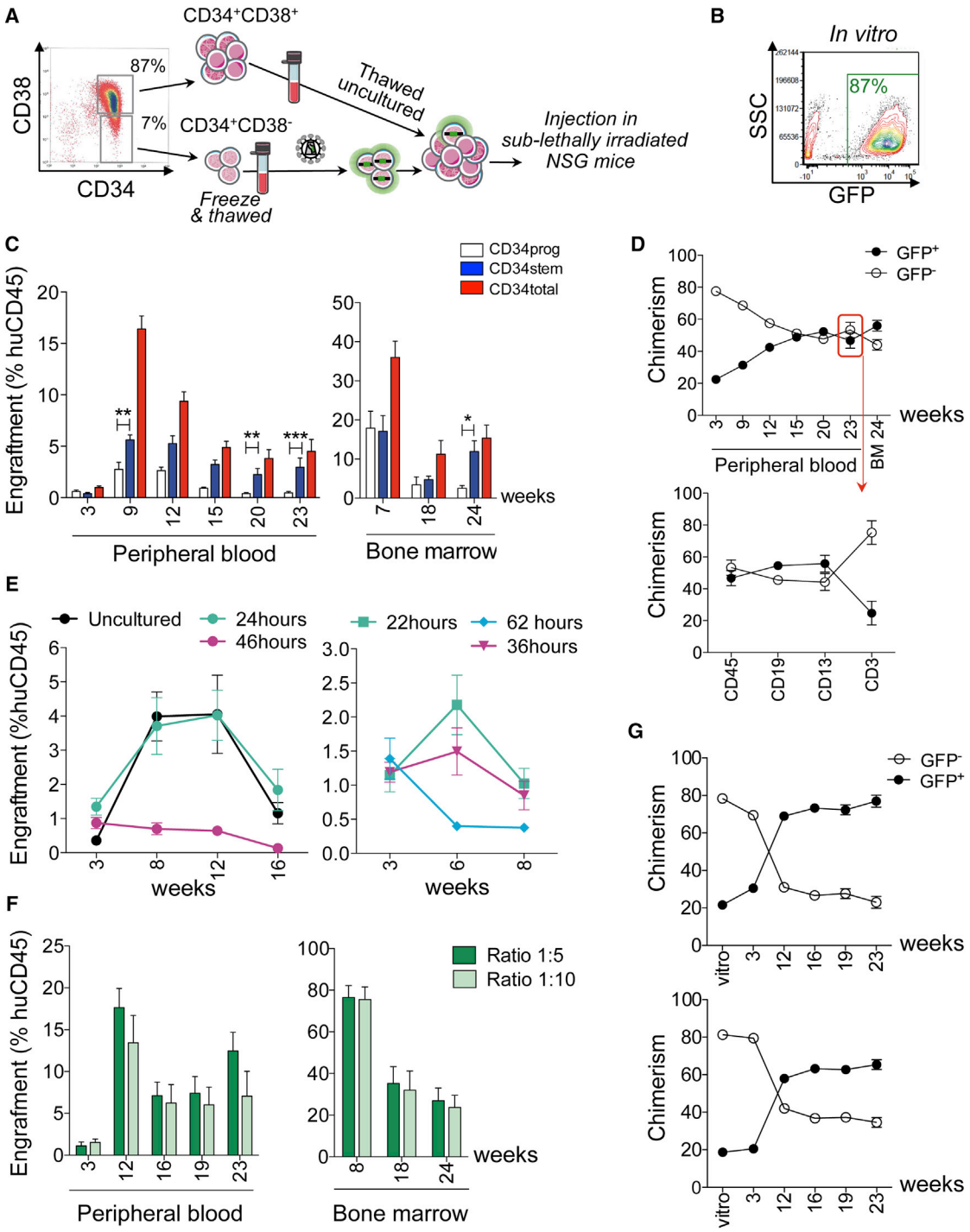

Figure 2. Co-transplantation of Gene-Modified, Long-Term Repopulating Cells with Uncultured Short-Term Progenitors

(A) Batches of $CD34^+CD38^+$ and $CD34^+CD38^-$ cells were generated and cryopreserved. As shown in the scheme, $CD34^+CD38^-$ ($CD34^{stem}$) cells were LV transduced and xenotransplanted with or without uncultured $CD34^+CD38^+$ ($CD34^{prog}$) cells.

(B) Representative transduction efficiency of $CD34^+CD38^-$ cells, as measured in the myeloid progeny after 14 days of culture.

(C) Human $CD45^+$ cell engraftment in PB and BM following transplantation of 50,000 GFP LV-transduced $CD34^{stem}$ cells (46 hr culture protocol; n = 5 mice), 350,000 uncultured $CD34^{prog}$ cells (n = 5 mice), or a mix of both ($CD34^{total}$ cells, stem:prog ratio 1:8; n = 6 mice). Significant differences with respect to the $CD34^{stem}$ group are shown (two-way ANOVA with Bonferroni's multiple comparison test).

(legend continued on next page)

potential extinguished thereafter, with persistence of low lymphoid (mostly T cell) engraftment at the latest time of analysis (Figures 1E and S1E). Within the $CD34^{prog}$ populations, almost no engraftment was derived from the highest CD38 subset, while short-term engraftment (3 weeks) was equally derived from $CD38^{int}$ and $CD38^{low}$ cells (Figures 1F and S1F). Within the $CD34^{total}$ population, the dominance of the $CD34^{+}CD38^{-}$ fraction in mediating nearly all multi-lineage long-term engraftment became evident at 9–10 weeks post-transplant (Figures 1F and S1F). We reached similar conclusions for BM-derived $CD34^{+}$ cells (Figure S2) and CB cells, where separation into $CD38^{+}$ and $CD38^{-}$ fractions was carried out with a bead-based sorting procedure (Figure S3).

A common practice to further enrich for engrafting HSCs is to purify the $CD90^{+}$ fraction of $CD34^{+}CD38^{-}$ HSPCs. We thus sought to define the engraftment kinetics of $CD90^{+/-}$ subpopulations of short-term ($CD34^{+}CD38^{low/int}$) or long-term ($CD34^{+}CD38^{-}$) repopulating HSPCs using a similar marking/re-assembly approach (Figure 1G). Again, long-term engraftment was almost exclusively derived from $CD34^{+}CD38^{-}$ cells. However, approximately one-third originated from the $CD90^{-}$ compartment, indicating that $CD90^{-}$ HSCs contribute to a substantial fraction of the severe combined immunodeficient mouse-repopulating cell (SRC) pool in mPB HSPCs (Figure 1G). CD90 was also expressed on 20%–30% of $CD34^{+}CD38^{+}$ progenitors, correlated with lower CD38 expression, and defined a population of short-term repopulating HSPCs that showed kinetics similar to $CD38^{low}$ cells.

A Gene Therapy Protocol Based on Transducing Purified HSCs

Our modeling suggested that $CD34^{+}CD38^{-}$ cells could substitute $CD34^{+}$ cells currently used in gene therapy trials when long-term correction of a genetic defect is the ultimate goal. However, $CD38^{int}$ cells may be critical for timely hematopoietic reconstitution following myeloablative conditioning. We therefore simulated a clinical scenario addressing this potential issue by co-transplanting gene-modified $CD34^{+}CD38^{-}$ ($CD34^{stem}$) cells with uncultured $CD34^{+}CD38^{+}$ ($CD34^{prog}$) cells in our xenograft model (Figure 2A). MPB-derived $CD34^{stem}$ cells were transduced with a GFP-expressing vector under saturating conditions resulting in >85% transduction efficiency in vitro (Figure 2B). Mice received either an ex-vivo-modified $CD34^{stem}$ graft, an uncultured $CD34^{prog}$ graft, or a total $CD34^{+}$ ($CD34^{total}$) graft re-assembled from the aforementioned two components ($CD34^{stem}$:$CD34^{prog}$ ratio 1:8). Surprisingly, we found that the $CD34^{prog}$ fraction persisted longer and even retained some long-term repopulating potential. Human cell chimerism of the re-assembled sample was approximately the sum of the $CD34^{stem}$ and $CD34^{prog}$ groups (Figure 2C) and GFP^{+} cell chimerism in the re-assembled graft stabilized around 50% in all lineages except T cells, where the $CD34^{prog}$ contribution was higher (Figure 2D). This result is in contrast to the experiments described in Figure 1, where similar sorting gates and transduction conditions have been used, except for the transplantation of cultured versus uncultured $CD34^{prog}$ cells.

These data suggest that fresh $CD34^{prog}$ cells (likely, within the $CD38^{low}$ cell fraction) contain some long-term repopulating capacity, which is lost during 2 days of ex vivo culture. To directly test this hypothesis, we xenotransplanted mPB $CD34^{prog}$ cells (the same donor and sorted aliquot as in the experiment shown in Figures 2B–2D) that were either uncultured, or cultured and transduced with a GFP LV during a 24 hr or a 48 hr ex vivo protocol. While engraftment at 3 weeks was similar or slightly better for the cultured cells, the 46 hr ex vivo group showed no short- or long-term engraftment thereafter, at variance to the uncultured group (Figure 2E). Interestingly, the shorter 24 hr ex vivo culture time restored engraftment potential to similar levels seen in uncultured cells. We repeated the experiment with $CD38^{prog}$ cells from a different donor, confirming that short-term engraftment potential starts to decrease after 36 hr of culture (Figure 2E). These findings provide a strong rationale to reduce ex vivo culture times to improve progenitor cell potency in gene therapy products.

(D) Top: GFP^{+} and GFP^{-} cell chimerism in PB and BM within the human $CD45^{+}$ cell compartment following transplantation of $CD34^{total}$ cells. Red arrow: GFP^{+}/GFP^{-} cell chimerism in $CD19^{+}$ B cells, $CD13^{+}$ myeloid cells, and $CD3^{+}$ T cells (PB, 23 weeks post-transplant).
(E) Left: mice were xenotransplanted with $CD34^{+}CD38^{+}$ cells that were uncultured (n = 4 mice), or cultured for 24 hr (n = 5 mice) or 46 hr (n = 4 mice) under standard conditions. Human $CD45^{+}$ cell engraftment in the PB is shown. Right (replicate experiment): PB engraftment of $CD34^{+}CD38^{+}$ cells cultured for 22 hr (n = 4 mice), 36 hr (n = 6 mice), or 62 hr (n = 3).
(F) Mice were xenotransplanted with $CD34^{total}$ cells composed of 50,000 GFP LV-transduced $CD34^{stem}$ cells (24 hr ex vivo protocol, no IL-3) and 200,000 uncultured $CD34^{prog}$ cells (ratio 1:5, n = 5 mice) or 450,000 uncultured $CD34^{prog}$ cells (ratio 1:10, n = 6 mice). Human $CD45^{+}$ cell engraftment in PB and BM is shown.
(G) GFP^{+} and GFP^{-} cell chimerism of the transplanted $CD34^{total}$ cells (in vitro) or the resulting human $CD45^{+}$ cell graft in the PB at the indicated time points post-transplant for the 1:5 (top) or 1:10 (bottom) stem:prog ratio.
Error bars represent SEM.

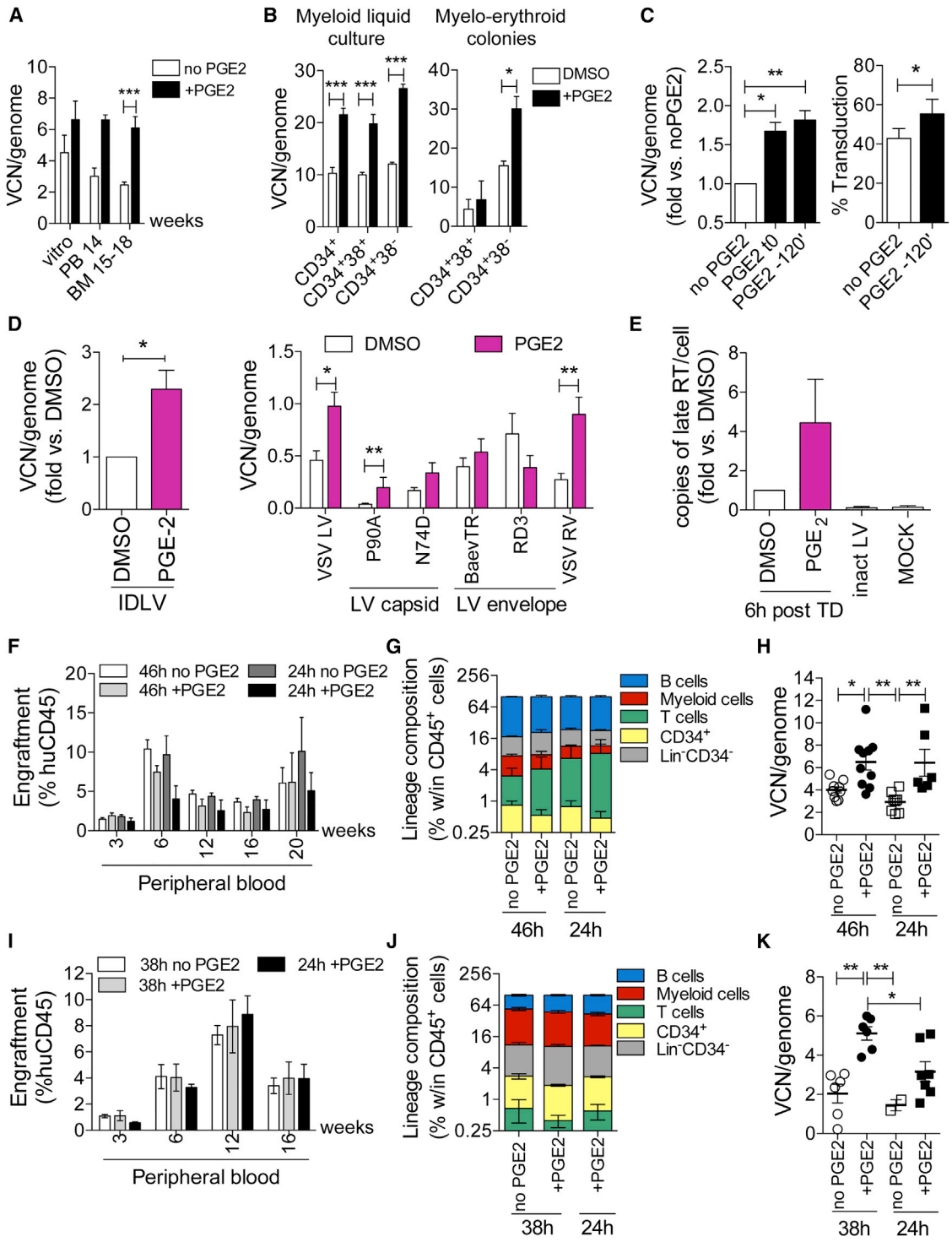

Figure 3. Prostaglandin E_2 Enables Efficient HSC Transduction with Shortened Ex Vivo Protocols

(A) CB $CD34^+$ cells were transduced with LVs in the presence or absence of 10 μM PGE_2. VCN was measured in the progeny after >7 days culture (n = 5) or in the human $CD45^+$ cell xenograft harvested from the PB (n = 2 experiments, blood from individual mice was pooled) or BM (2 experiments, n = 13 mice in the no PGE_2 group, n = 10 mice in PGE_2 group, statistics by Student's t test).

(legend continued on next page)

We thus reasoned that $CD34^{stem}$ HSPCs might better compete with uncultured progenitor cells when their ex vivo culture is reduced to 24 hr. In addition, we eliminated interleukin-3 (IL-3) from the culture medium, given that it stimulates progenitors rather than HSCs and has recently been implicated in accelerated loss of short-term repopulation potential (Miller et al., 2016). Using mPB $CD34^{stem}$ and $CD34^{prog}$ aliquots from the same donor and a sorting strategy as in the experiment shown in Figures 2B–2D, we co-transplanted mPB $CD34^{stem}$ cells transduced with GFP LV according to the optimized and shortened ex vivo protocol with uncultured $CD34^{prog}$ cells mixed in a 1:5 ratio or a 1:10 ratio. The fraction of GFP^+ cells scored in vivo was used as a surrogate marker for $CD34^+CD38^-$-derived hematopoiesis, assuming that most $CD34^{stem}$ cells were transduced even under the shortened 24 hr ex vivo culture protocol. Engraftment levels were similar between the 1:5 and 1:10 groups (Figure 2F). Importantly, up to 80% and 70% of hematopoietic progeny were stably gene marked in vivo, respectively, and equilibrium was reached between 3 and 4 months post-transplantation (Figure 2G). We conclude that shortening the culture time of $CD34^+CD38^-$ cells to 24 hr in an IL-3-free medium significantly enhanced progenitor fitness within the gene-modified $CD34^+CD38^-$ cells allowing a contribution of up to 80% of the long-term graft even when large amounts of uncultured $CD34^+CD38^+$ progenitor cells were co-infused.

Robust HSC Gene Transfer Using Short Culture Time and Prostaglandin E_2

To date, most clinical protocols employ culture times of more than 60 hr and multiple exposures to LV (in general, two transduction cycles). Therefore, a significant challenge when implementing shorter transduction protocols in the clinic is to achieve sufficiently high levels of gene transfer with large-scale LV preparations produced under good manufacturing practice (GMP). Unexpectedly, we found that the more primitive $CD34^+CD38^-$ cells were transduced to almost 2-fold-higher vector copy number per genome (VCN) than the more committed counterparts after a single LV exposure (Figure S4). This phenomenon may facilitate gene transfer when manipulating more purified HSC populations.

Furthermore, we sought to enhance transduction by small-molecule compounds. While employing 16,16-dimethyl prostaglandin E_2 (PGE_2) as an anti-apoptotic agent in ex vivo HSC gene-editing protocols, we noted that it increased gene-targeting efficiency (Genovese et al., 2014). We hypothesized that PGE_2 may also increase transduction by integrating LV. Indeed, pre-stimulating CB $CD34^+$ HSPCs with 10 μM PGE_2 before transduction increased VCN in the progeny ~1.5-fold in vitro, an increase that was maintained or increased after xenotransplantation (Figure 3A). PGE_2 also enhanced transduction of $CD34^+$ cells from BM (Figure 3B), including the more primitive $CD34^+CD38^-$ subset, and mPB, whereby the

(B) BM $CD34^+$ subpopulations (n = 3 donors) were transduced with GFP LV (MOI = 100) + 10 μM PGE_2 or DMSO, and VCN was measured in the myeloid progeny after 14 days of culture or on myelo-erythroid colonies obtained from clonogenic assay. Statistics by two-way ANOVA with Bonferroni's multiple comparison test.
(C) mPB $CD34^+$ cells (n = 8 donors) were transduced with GFP LV (38 hr protocol) ± 10 μM PGE_2 added at the beginning of culture (t0) or during pre-stimulation, 120 min before LV addition (−120′). Transduction was evaluated after 14 days in culture. Left: VCN relative to the no PGE_2 group (statistics by Wilcoxon signed rank test). Right: transduction efficiency measured by flow cytometry (n = 6) (statistics by Student's t test).
(D) mPB $CD34^+$ cells (n = 3 donors, with two replicates each) were transduced with GFP-expressing LV variants after adding PGE_2 or DMSO (−120′). IDLV, integrase-deficient, VSV-G pseudotyped LV; VSV LV, integration-competent, VSV-G-pseudotyped LV; P90A and N74D, VSV-G-pseudotyped LV with capsid mutants; BaEV-TR and RD114-TR, integration-competent LV pseudotyped with the BaEV-TR and RD114-TR envelopes, respectively. VCN were measured by specific droplet digital PCR assays. Statistics were performed by Mann-Whitney test.
(E) Quantification of late reverse-transcription DNA intermediates (late-RT) in mPB $CD34^+$ cells (n = 6 donors), 6 hr after transduction (TD) in PGE_2 or DMSO.
(F–H) mPB $CD34^+$ cells were transduced with $gp91^{phox}$-expressing LVs (MOI = 100) using a 24 or 46 hr ex vivo protocol ± 10 μM PGE_2, and xenotransplanted with the day 0 equivalent of 500,000 cells (n = 6–9 mice/group). (F) Human $CD45^+$ cell engraftment in the PB. (G) Lineage composition of the human $CD45^+$ cell graft in the BM at 20 weeks post-xenotransplantation. B cells, $CD19^+$; myeloid cells: $CD33^+$; T cells: $CD3^+$; $CD34^+$: HSPCs; Lin^-CD34^-: $CD19^-$ $CD33^-CD3^-CD34^-$ cells. (H) VCN in the human graft recovered from the BM at 20 weeks post-xenotransplantation. Statistics by one-way ANOVA with Bonferroni's multiple comparison test.
(I–K) mPB $CD34^+CD38^-$ cells were transduced with purified Globe LV (MOI = 100) using a 24 or 38 hr ex vivo protocol ±10 μM PGE_2, and xenotransplanted with the day 0 equivalent of 50,000 cells (experiment 1: 38 hr no PGE_2, n = 4; 38 hr + PGE_2, n = 4; 24 hr + PGE_2, n = 5; experiment 2: 38 hr no PGE_2, n = 4; 38 hr + PGE_2, n = 4; 24 hr no PGE_2, n = 5; 24 hr + PGE_2, n = 4). (I) Human $CD45^+$ cell engraftment in the PB. (J) Lineage composition of the human $CD45^+$ cell graft in the BM at 20 weeks post-xenotransplantation (representative mice from experiment 1). (K) VCN in the human graft recovered from the BM at 18 weeks (experiment 2) or 20 weeks (experiment 1) post-xenotransplantation. Statistics by one-way ANOVA with Bonferroni's multiple comparison test.
Error bars represent SEM. See also Figure S4.

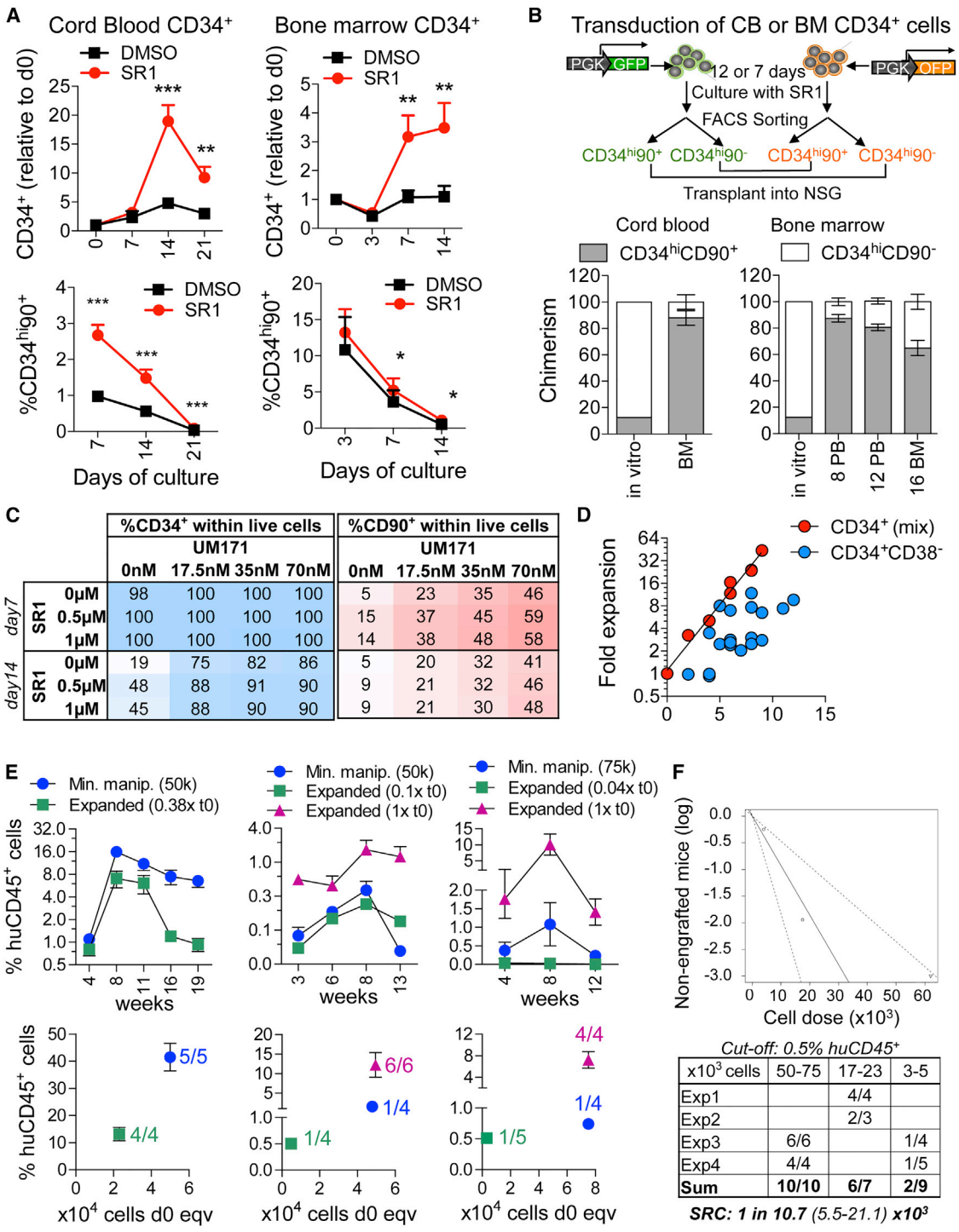

Figure 4. Ex Vivo Expansion of Gene-Modified HSCs Supported by Small-Molecule Compounds

(A) LV-transduced CB (left panel, n = 6 donors) or BM (right panel, n = 5 donors) $CD34^+$ HSPCs were expanded ex vivo in the presence of vehicle (DMSO) or StemRegenin 1 (SR1, 1 µM), as described by Boitano et al. (2010). The fraction of $CD34^{high}CD90^+$ cells in the culture at the indicated number of days is shown (statistics by matched two-way ANOVA with Bonferroni's multiple comparison test).

(B) CB or BM $CD34^+$ cells were divided into equal fractions and transduced with GFP- or OFP- expressing LVs. GFP^+ and OFP^+ cells were expanded for 12 days (CB) and 7 days (BM) in the presence of SR1, followed by sorting of each group into a $CD34^{high}CD90^+$ and $CD34^+CD90^-$ fractions. Each GFP^+ fraction was then re-combined with the complementary OFP^+ $CD34^+$ cell fraction and xenotransplanted. The fraction of

(legend continued on next page)

timing of PGE_2 stimulation was flexible (Figure 3C). At non-saturating LV doses, PGE_2 also increased the fraction of transduced cells, not only VCN (Figure 3C). We then tested whether PGE_2 increased transduction by vector variants to determine a mechanism of action. Gene transfer was increased when using vesicular stomatitis virus G protein (VSV-G)-pseudotyped, integrase-deficient LV, or gamma-retroviral vectors, and also in the case of HIV1 capsid mutants that reduce interaction with cyclophilin A (P90A) or CPSF6 (N74) during uncoating (Figure 3D). On the other hand, when pseudotyping LVs with alternative, non-endocytosis-dependent envelopes, we could not appreciate a significant impact of PGE_2 on transduction. Quantification of reversely transcribed vector DNA intermediates 6 hr post-transduction further indicated that PGE_2 acted during the early steps of transduction (Figure 3E).

We then performed in vivo repopulation assays on $CD34^+$ mPB cells transduced in the presence or absence of PGE_2 using either a 46 hr or an ultra-short 24 hr ex vivo culture protocol. Despite injecting fewer cells in the 24 hr protocol groups (the yield of 500,000 plated $CD34^+$ cells was lower after 24 hr with respect to 46 hr, because of less proliferation during the shorter ex vivo culture), $huCD45^+$ cell engraftment was equivalent to the 46 hr protocol (Figure 3F). PGE_2 treatment had no overall effect on ex vivo proliferation, colony-forming potential (Figure S4D), or engraftment levels (Figure 3F), nor did it alter the lineage composition of the human graft (Figure 3G). At the experimental endpoint (20–24 weeks post-transplant), we noted significantly higher VCN in the PGE_2 groups (Figure 3H).

Next, we transduced $CD34^+CD38^-$ mPB cells with a purified LV expressing a therapeutic gene. We tested the impact of PGE_2 on gene transfer efficiency in the context of a short 38 hr or an ultra-short 24 hr ex vivo culture protocol. In vitro results of VCN in liquid cultures established from $CD34^+CD38^-$ cells showed that exposure to PGE_2 doubled VCN (Figure S4E). Following transplantation, we detected no statistically significant differences in engraftment or graft composition (Figures 3I and 3J). Importantly, differences in VCN were maintained in the human graft at 18–20 weeks post-transplant, confirming that PGE_2 increased gene transfer into long-term repopulating cells (Figure 3K).

Taken together, these results suggest that a minimal ex vivo manipulation protocol, as short as 24 hr, can achieve substantial levels of gene transfer by therapeutic LVs in human HSCs from clinically relevant sources. The effect of PGE_2 was particularly robust for the 38 hr protocol in $CD34^+CD38^-$ cells, motivating its clinical implementation.

Ex Vivo Expansion of $CD34^+CD38^-$ Cells from mPB in the Presence of Pyrimidoindole Derivatives

Based on our finding that short-term engrafting cells are particularly sensitive to ex vivo culture, we hypothesized that HSC expansion protocols could be more suitably applied to highly purified HSC fractions. First, we set out to functionally validate surface markers that prospectively identify SRC after 1–2 weeks of expansion culture. BM or CB $CD34^+$ cells were cultured in the presence or absence of the arylhydrocarbon receptor antagonist StemRegenin 1 (SR1) (Boitano et al., 2010). Serial flow cytometric analysis indicated that CD38 expression was rapidly lost in culture, while a fraction of cells maintained a $CD34^{high}CD90^+$ phenotype. This fraction was higher when cells were cultured with SR1, especially for CB (Figure 4A). Peak expansion of $CD34^{high}CD90^+$ cells occurred around 2 weeks for CB and 1 week for BM. In a separate experiment, we transduced 50% of CB or BM $CD34^+$ cells with a GFP-expressing LV, while the other 50% were transduced with an OFP-expressing LV. Both GFP^+ and OFP^+ cells were expanded for 12 days (CB) or 7 days (BM) in the presence of

$CD34^{hi}CD90^+$ cells in vitro after re-combining, as well as the in vivo output deriving from this fraction tracked by expression of the associated FP (CB $CD34^+$ cells: BM at 20 weeks post-xenografting; BM $CD34^+$ cells: PB and BM up to 16 weeks) are shown. CB, n = 6 mice; BM, n = 6 mice.

(C) mPB $CD34^+CD38^-$ cells were expanded ex vivo in the presence of increasing concentrations of SR1, UM171 or combinations of both. Reported are the percentages of $CD34^+$ and $CD90^+$ cells in the culture at 7 and 14 days.

(D) Growth kinetics of total $CD34^+$ versus $CD34^+CD38^-$ mPB cells expanded in the presence of UM171 (35 nM).

(E) mPB $CD34^+CD38^-$ cells were LV transduced and xenotransplanted after <36 hr ex vivo (minimally manipulated cells, 50,000–75,000 cells/mouse) or after an additional 7–8 days of expansion in 35 nM UM171. Injected cell dose is indicated relative to the minimally manipulated cell dose (t0 equivalent). Upper graphs show the percentage of $huCD45^+$ cells in the PB. Lower graphs show BM engraftment relative to administered cell dose (t0 cell equivalents) at the experimental endpoint, 20 weeks (left) or 13–14 weeks (middle and right graphs) post-transplant. The number of engrafted mice (>0.5% $huCD45^+$ and both myeloid and lymphoid reconstitution in BM at the endpoint) is indicated.

(F) Estimation of SRC frequency in ex-vivo-expanded $CD34^+CD38^-$ cells by extreme limiting dilution statistics, considering the t0 cell dose equivalents (62,500–20,000–4,000) transplanted in four independent experiments (Exp).

Error bars represent SEM.

SR1. To test whether CD90 expression could be useful to enrich for engrafting cells following prolonged ex vivo culture, we sorted the cultures into $CD34^{high}CD90^{+}$ or $CD34^{high}CD90^{-}$ fractions, mixed the $GFP^{+}CD90^{+}$ cells with the $OFP^{+}CD90^{-}$ cells and vice versa without altering their original ratio ($CD90^{+}$ cells constituted 10%–20% of the $CD34^{high}$ cells or 1%–5% of the total cells) and xenotransplanted them (Figure 4B). Both for CB and BM, most long-term engraftment derived from the $CD34^{high}CD90^{+}$ fraction.

Using the CD34 and CD90 markers as surrogates for SRC, we next screened different expansion conditions for mPB $CD34^{+}CD38^{-}$ cells by varying the concentrations of SR1 and/or the pyrimidoindole derivative UM171 (Fares et al., 2014). Notably, $CD34^{+}CD38^{-}$ cells proliferated little during the first week and homogeneously maintained CD34 expression. UM171 substantially increased the fraction and number of $CD90^{+}$ cells over control cultures or cells cultured with SR1, while combination of UM171 and SR1 had additive effects during the first week of culture (Figure 4C). We then compared the growth characteristics of transduced $CD34^{+}$ and $CD34^{+}CD38^{-}$ mPB cells during expansion culture (Figure 4D). $CD34^{+}CD38^{-}$ cells generally showed little growth in the first days of ex vivo culture and then expanded at variable rates, which differed by donor and experiment. On the other hand, $CD34^{+}$ cells steadily duplicated every 2 days, likely reflecting the progenitors responding to cytokine stimulation. This overgrowth of progenitors rapidly drove up culture volumes while keeping the concentration of $CD34^{+}$ cells stable, highlighting a substantial practical advantage of the $CD34^{+}CD38^{-}$ cultures. To functionally test the repopulation potential of UM171-expanded, genetically engineered HSPCs, we xenotransplanted LV-transduced $CD34^{+}CD38^{-}$ cells either after a minimal, 24–36 hr ex vivo culture (minimally manipulated cells) or after an additional 7–8 days of ex vivo expansion (Figure 4E). When matching transplanted cell number according to the same "t0 equivalent" (1× t0), we found higher engraftment in the ex vivo expanded sample (Figure 4E, pink dots). When the transplanted cell dose was matched according to the post-culture counts, ex vivo expanded cells showed lower engraftment compared with minimally manipulated cells, consistent with the 3- to 25-fold lower "t0 equivalent" cell dose (0.38–0.04× t0) injected (Figure 4E, green dots). To estimate the frequency of SRC in UM171-expanded $CD34^{+}CD38^{-}$ HSPCs, we performed limiting-dilution statistics on the "t0 equivalent" cell doses that were transplanted in four replicate experiments (Figure 4F). Estimated SRC frequency was 1 in 10,700 (95% confidence interval: 5,500–21,100), which compares with a recently reported SRC frequency of ~1 in 141,203 in uncultured $CD34^{+}$ cells from G-CSF-mPB (Lidonnici et al., 2016). Taken together, these data indicate that our protocol allows ex vivo expansion of genetically engineered mPB $CD34^{+}CD38^{-}$ cells with SCID-repopulating potential and warrants further protocol optimization for clinical application.

DISCUSSION

Transplantation of genetically engineered, autologous HSPCs is emerging as a less risky and potentially more efficacious alternative to allogeneic transplantation for a series of non-malignant indications (Naldini, 2015). To fully harness the advantages of gene therapy, genetic engineering of HSPCs must be developed into a standardized and sustainable method. To reach this objective, key challenges include improving LV transduction, minimizing the negative impact of ex vivo culture to ensure faster and more polyclonal long-term reconstitution, and alleviating the safety concerns related to insertional mutagenesis. Here we developed a series of readily translatable strategies that overcome these hurdles and help to establish gene therapy as a widely available standard treatment.

We revealed the PGE_2-enhanced transduction of human HSPCs by VSV-G-pseudotyped LV, possibly by acting on the endocytosis-dependent entry pathway. Applying PGE_2 makes shorter ex vivo manipulation protocols that feature a single transduction cycle clinically viable, mitigating the negative effect of prolonged culture on progenitor cell engraftment and allowing to double the number of patients that can be treated with a given vector batch with respect to current clinical standards. Importantly, the enhancing effect of PGE_2 on LV transduction has recently been reported by an independent group (Heffner et al., 2016). In contrast to other pharmacological interventions that enhance transduction but may also have broader effects on HSC biology and/or cause toxicity (Wang et al., 2014; Petrillo et al., 2015), PGE_2 was non-toxic, did not change the biological properties of the cells, and has already been safely employed in an ex vivo setting to increase CB engraftment in patients (Cutler et al., 2013). We did not note a significant increase in engraftment levels in the PGE_2 groups, as could be expected from published data (Goessling et al., 2011). Further studies on diverse cell sources employing ultra-short ex vivo protocols are warranted to understand whether the promoting effects of PGE_2 on LV transduction and engraftment capacity are functionally linked to a common mechanism and whether both effects can be exploited contemporaneously. The shortened PGE_2 protocol can be readily applied to current ex vivo gene therapy trials and should translate clinically into accelerated hematologic recovery.

We provide evidence here that $CD34^{+}CD38^{-}$ cells transduce at higher levels than total $CD34^{+}$ cells, consistent

with a recent report (Baldwin et al., 2015). In vitro, the effect was most robust (1) when cell populations were sorted before transduction (Figure S4C), (2) when saturating vector doses were used (Figure S4B), and (3) when PGE_2 was employed (Figure 3B). We hypothesize that the lack of cell division of $CD34^+CD38^-$ cells during the first days of culture (Figure 4F) may give more time for infecting LV to complete integration before DNA replication, thus transmitting a copy of each provirus to both daughter cells, whereas the rapidly dividing $CD38^+$ progenitors may randomly sort the LV pre-integration complexes between the two daughter cells. Considering that PGE_2 relieves an early transduction block, applying it to purified $CD34^+CD38^-$ cells may provide added benefits in terms of gene transfer efficiency. Robust gene transfer into HSCs may allow reducing the intensity of the conditioning regimen and implementing non-genotoxic and stem cell-specific conditioning strategies (Palchaudhuri et al., 2016). Regarding safety, avoiding the infusion of $CD38^+$ progenitors carrying semi-random LV integrations would reduce the integration load 10-fold, thereby decreasing the chances of gain-of-function events due to insertional mutagenesis, which may originate from immortalized progenitor cells (Cavazzana-Calvo et al., 2010; Stein et al., 2010; Braun et al., 2014).

We argue that gene therapy based on transduced, purified $CD34^+CD38^-$ cells is clinically feasible and offers advantages over alternative strategies that have previously been employed in clinical trials to obtain HSC-enriched cell populations, including positive selection for $CD133^+$ cells (Gordon et al., 2003) or $CD34^+CD90^+$ cells (Michallet et al., 2000; Negrin et al., 2000). Combining a negative (CD38) with a positive (CD34) selection marker allows using a sequential, bead-based selection procedure that can be made GMP compliant and implemented in centers that already possess standard cell separation equipment. The 10-fold gain in HSC purity with respect to $CD34^+$ cells is higher than what can be achieved with the $CD133^+$ (2×) or the $CD34^+CD90^+$ (up to 5×) selection strategies. Furthermore, we show that almost all long-term repopulation activity is captured within the $CD34^+CD38^-$ fraction, while, in agreement with CB data (Notta et al., 2011), substantial numbers of HSCs are contained within the $CD34^+CD90^-$ fraction of mPB, which would be discarded in the case of a $CD34^+CD90^+$ selection. While more stringent gating on $CD90^{high}$ cells may increase HSC purity, it would at the same time aggravate the loss of $CD90^{-/low}$ HSCs.

Our functional analyses showed that CD38 expression inversely correlated with time of onset and persistence of the graft, confirming and extending published results obtained in xenograft models (Glimm et al., 2001; Kerre et al., 2001; Mazurier et al., 2003). Interestingly, analysis of clonal dynamics by LV integration sites in a clinical gene therapy trial pointed to two distinct waves of repopulation, switching between the third and sixth month post-transplant, which may correspond to the waves generated by $CD34^+CD38^{int/+}$ and $CD34^+CD38^-$ cells, respectively (Biasco et al., 2015). Transplantation of genetically engineered $CD34^+CD38^-$ cells may repopulate patients following the kinetics of the second wave resulting in a fully established transgenic hematopoiesis beyond 3 months after transplantation. While this may be suboptimal for genetic diseases with an urgent transplant indication such as PIDs, it may be acceptable for chronic conditions such as hemoglobinopathies. Considering the timing of repopulation by $CD34^+CD38^-$ cells, co-infusion of progenitor cells is advisable when a fully myeloablative conditioning regimen is applied to facilitate short-term engraftment. These short-term engrafting progenitors can be conveniently obtained from the $CD38^{int/+}$ fraction left over from the negative selection step and cryopreserved as a whole, without further ex vivo manipulation. Infusing uncultured progenitors may be particularly beneficial for hematologic recovery, considering their selective vulnerability to ex vivo culture. Low CD38 expression on CB HSPCs has been associated with stem cell activation and recruitment into the G1 phase of the cell cycle (McKenzie et al., 2007). Unbalanced stimulation by high doses of cytokines may irreversibly push these cells to differentiate resulting in a loss of self-renewal potential and premature exhaustion in vivo.

On the contrary, the more primitive $CD34^+CD38^-$ mPB cells appeared to be more tolerant to ex vivo culture. Using the shortened transduction protocol, we effectively alleviated competition from a 10-fold excess of uncultured progenitors. Moreover, we demonstrate that, with the help of the pyrimidoindole derivative UM171 (Fares et al., 2014), the culture time of mPB $CD34^+CD38^-$ cells can extend beyond 7 days, with evidence for SRC expansion. We foresee numerous applications for ex vivo expansion of postnatally derived HSCs in the gene therapy field. This technology can overcome disease- or patient-specific cell shortages, allow more complex genetic manipulations such as serial transductions by multiple vectors, possibly with selection of engineered cells, and enable therapeutic application of emerging gene-editing technologies (Naldini, 2015). The use of purified $CD34^+CD38^-$ cells and the associated reduction in culture volumes and vector amount promises substantial cost savings and quality improvements, also considering that differentiating progenitor and mature cell populations may give rise to inhibitory feedback and differentiation signaling exhausting the long-term repopulating potential of the more primitive cells in the culture (Csaszar et al., 2012).

In conclusion, our data support the stepwise introduction of incremental improvements in the ex vivo HSPC

engineering process into clinical testing, ultimately fulfilling the promise of gene therapy to the community.

EXPERIMENTAL PROCEDURES

Mice

NOD.Cg-Prkdc^{scid}IL2rg^{tm1Wjl}/SzJ (NSG) mice were acquired from the Jackson Laboratory. All animal procedures were performed according to protocols approved by the Institutional Animal Care and Use Committee (IACUC 618) and communicated to the Ministry of Health and local authorities according to the Italian law. Eight week old mice were sublethally irradiated (200–220 cGy) and transplanted with human HSPCs by tail vein injection. All mice were randomized into different HSC transplantation groups. On the basis of a standard backward sample size calculation, we transplanted at least three to ten mice per condition and performed at least two independent experiments to obtain a sufficient number of mice to perform statistical analysis. Human cell engraftment was blindly assessed by serial bleeding or BM aspirates, as described in the Supplemental Experimental Procedures.

Procurement, Culture, and Transduction of Human HSPCs

Human CB, BM, or mPB was purchased from commercial sources (Lonza, HemaCare, or All Cells). CD34$^+$ or CD34$^+$CD38$^-$ cells were pre-stimulated in serum-free medium supported with early-acting human cytokines (SCF, FLT3L, or TPO with or without IL-3 or IL-6), and transduced with concentrated LV at an MOI of 100, unless otherwise indicated. Where indicated, 10 μM 16,16-dimethyl-prostaglandin E_2 (Cayman Chemical) was added before LV transduction. Additional details can be found in the Supplemental Experimental Procedures.

Cell Sorting and Flow Cytometry

Sorting for CD34$^+$ cells (and CD38$^-$ cells, where indicated) was performed by magnetic beads (Miltenyi). Fluorescence-activated cell sorting for CD38 and CD90 subpopulations was performed on a MoFlo XDP sorter (Beckman Coulter). Analytical flow cytometry was performed on a FACSCanto II or LSR II Fortessa instrument (BD Bioscience). Details on protocols and reagents can be found in the Supplemental Experimental Procedures.

Ex Vivo HSPC Expansion

Expansion cultures were set up in serum-free medium (StemSpan, STEMCELL Technologies or StemMacs, Miltenyi) containing, unless otherwise indicated, 100 ng/mL SCF, 100 ng/mL FLT3L, 50 ng/mL TPO, 50 ng/mL IL-6, 35 nM UM171 (STEMCELL Technologies), and/or 1 μM SR1 (BioVision Technologies). Starting cell density was 1×10^5 cells/mL, and fresh medium was manually added as needed, to keep cell concentration always below 1×10^6 cells/mL. Cultures were kept at 37°C, 5% CO_2 under normoxia.

LV Production, Titration, and Molecular Analysis of Gene Transfer Efficiency

Purified vectors (Globe LV, some batches of PGK.GFP LV) were produced and titered by MolMed, according to the GMP process employed in our clinical trials (Biffi et al., 2013; Aiuti et al., 2013). Lab-grade vectors were produced and titered on 293T cells according to standard lab protocols, as described previously. Molecular quantification of gene transfer efficiency was performed using specific qPCR assays, as detailed in the Supplemental Experimental Procedures.

Statistical Analysis

In all studies, values are expressed as means ± SEM, unless otherwise indicated. Statistical analyses were performed by Mann-Whitney test, Student's t test, Wilcoxon signed rank test, or ANOVA test as indicated. Percentages were converted into log odds for statistical analysis. Significance levels are coded as follows throughout the manuscript: *$p < 0.05$, **$p < 0.01$, ***$p < 0.001$.

SUPPLEMENTAL INFORMATION

Supplemental Information includes Supplemental Experimental Procedures, four figures, and one table and can be found with this article online at http://dx.doi.org/10.1016/j.stemcr.2017.02.010.

AUTHOR CONTRIBUTIONS

E.Z. performed experiments, analyzed the data, and contributed to writing the manuscript. G.D., F.E.B., C.P., and M.R.L. performed experiments. A.K.R. provided intellectual input and supervised C.P. A.A. and G.F. provided intellectual input, reagents, and protocols. L.N. supported the project, provided research infrastructure, gave intellectual input, and edited the manuscript. B.G. designed and coordinated the research, analyzed the data, and wrote the manuscript.

ACKNOWLEDGMENTS

We thank Oriana Meo, Matteo Maria Naldini, Andrea Cosentino, Cheruku Patali Shikhi, Lucia Sergi Sergi, Ivan Cuccovillo, and Tiziana Plati for help with experiments; C. Villa, E. Canonico, M. Romanó, M. Zambelli, and C. Parisi for help with sorting and cell manipulation; MolMed S.p.A. for providing the lentiviral vector pseudotyped with RD114-TR envelope; François-Loic Cosset from Inserm-ENS Lyon, France, for the BaEV-TR envelope construct; Guy Sauvageau for friendly discussions on HSC expansion. This research was supported by grants from the Telethon Foundation (TELE16-C1 to B.G., TELE16-C3 to A.K.R.), the Telethon-GSK Alliance (AGSK-HSC), the Italian Ministry of Health (NET-2011-02350069) and a John Goldman Clinical Research Fellowship from the European Hematology Association to B.G.

Received: November 22, 2016
Revised: February 13, 2017
Accepted: February 13, 2017
Published: March 16, 2017

REFERENCES

Aiuti, A., Biasco, L., Scaramuzza, S., Ferrua, F., Cicalese, M.P., Baricordi, C., Dionisio, F., Calabria, A., Giannelli, S., Castiello, M.C.,

et al. (2013). Lentiviral hematopoietic stem cell gene therapy in patients with Wiskott-Aldrich syndrome. Science *341*, 1233151.

Baldwin, K., Urbinati, F., Romero, Z., Campo-Fernandez, B., Kaufman, M.L., Cooper, A.R., Maziuk, K., Hollis, R.P., and Kohn, D.B. (2015). Enrichment of human hematopoietic stem/progenitor cells facilitates transduction for stem cell gene therapy. Stem Cells *33*, 1532–1542.

Biasco, L., Pellin, D., Scala, S., Dionisio, F., Basso-Ricci, L., Leonardelli, L., Scaramuzza, S., Baricordi, C., Ferrua, F., Cicalese, M.P., et al. (2015). In vivo tracking of human hematopoiesis reveals patterns of clonal dynamics during early and steady-state reconstitution phases. Cell Stem Cell *19*, 107–119.

Biffi, A., Montini, E., Lorioli, L., Cesani, M., Fumagalli, F., Plati, T., Baldoli, C., Martino, S., Calabria, A., Canale, S., et al. (2013). Lentiviral hematopoietic stem cell gene therapy benefits metachromatic leukodystrophy. Science *341*, 1233158.

Boitano, A.E.A., Wang, J., Romeo, R., Bouchez, L.C., Parker, A.E., Sutton, S.E., Walker, J.R., Flaveny, C.A., Perdew, G.H., Denison, M.S., et al. (2010). Aryl hydrocarbon receptor antagonists promote the expansion of human hematopoietic stem cells. Science *329*, 1345–1348.

Braun, C.J., Boztug, K., Paruzynski, A., Witzel, M., Schwarzer, A., Rothe, M., Modlich, U., Beier, R., Göhring, G., Steinemann, D., et al. (2014). Gene therapy for Wiskott-Aldrich syndrome – long-term efficacy and genotoxicity. Sci. Transl. Med. *6*, 227ra33.

Cartier, N., Hacein-Bey-Abina, S., Bartholomae, C.C., Veres, G., Schmidt, M., Kutschera, I., Vidaud, M., Abel, U., Dal-Cortivo, L., Caccavelli, L., et al. (2009). Hematopoietic stem cell gene therapy with a lentiviral vector in x-linked adrenoleukodystrophy. Science *326*, 818–823.

Cavazzana-Calvo, M., Payen, E., Negre, O., Wang, G., Hehir, K., Fusil, F., Down, J., Denaro, M., Brady, T., Westerman, K., et al. (2010). Transfusion independence and HMGA2 activation after gene therapy of human β-thalassaemia. Nature *467*, 318–322.

Csaszar, E., Kirouac, D.C., Yu, M., Wang, W., Qiao, W., Cooke, M.P., Boitano, A.E., Ito, C., and Zandstra, P.W. (2012). Rapid expansion of human hematopoietic stem cells by automated control of inhibitory feedback signaling. Cell Stem Cell *10*, 218–229.

Cutler, C., Multani, P., Robbins, D., Kim, H.T., Le, T., Hoggatt, J., Pelus, L.M., Desponts, C., Chen, Y.B., et al. (2013). Prostaglandin-modulated umbilical cord blood hematopoietic stem cell transplantation. Blood *122*, 3074–3081.

Fares, I., Chagraoui, J., Gareau, Y., Gingras, S., Ruel, R., Mayotte, N., Csaszar, E., Knapp, D.J.H.F., Miller, P., Ngom, M., et al. (2014). Cord blood expansion. Pyrimidoindole derivatives are agonists of human hematopoietic stem cell self-renewal. Science *345*, 1509–1512.

Genovese, P., Schiroli, G., Escobar, G., Di Tomaso, T., Firrito, C., Calabria, A., Moi, D., Mazzieri, R., Bonini, C., Holmes, M.C., et al. (2014). Targeted genome editing in human repopulating haematopoietic stem cells. Nature *510*, 235–240.

Glimm, H., Oh, I.H., and Eaves, C.J. (2000). Human hematopoietic stem cells stimulated to proliferate in vitro lose engraftment potential during their S/G(2)/M transit and do not reenter G(0). Blood *96*, 4185–4193.

Glimm, H., Eisterer, W., Lee, K., Cashman, J., Holyoake, T.L., Nicolini, F., Shultz, L.D., Von Kalle, C., and Eaves, C.J. (2001). Previously undetected human hematopoietic cell populations with short-term repopulating activity selectively engraft NOD/SCID-2 microglobulin-null mice. J. Clin. Invest. *107*, 199–206.

Goessling, W., Allen, R.S., Guan, X., Jin, P., Uchida, N., Dovey, M., Harris, J.M., Metzger, M.E., Bonifacino, A.C., Stroncek, D., et al. (2011). Prostaglandin E2 enhances human cord blood stem cell xenotransplants and shows long-term safety in preclinical nonhuman primate transplant models. Cell Stem Cell *8*, 445–458.

Gordon, P.R., Leimig, T., Babarin-Dorner, A., Houston, J., Holladay, M., Mueller, I., Geiger, T., and Handgretinger, R. (2003). Large-scale isolation of CD133+ progenitor cells from G-CSF mobilized peripheral blood stem cells. Bone Marrow Transpl. *31*, 17–22.

Hacein-Bey Abina, S., Gaspar, H.B., Blondeau, J., Caccavelli, L., Charrier, S., Buckland, K., Picard, C., Six, E., Himoudi, N., Gilmour, K., et al. (2015). Outcomes following gene therapy in patients with severe Wiskott-Aldrich syndrome. JAMA *313*, 1550–1563.

Heffner, G., Bonner, M., Campbell, D., Christiansen, L., Pierciey, F.J., Zhang, W., Lewis, G., Smurnyy, Y., Hamel, A., Shah, S., et al. (2016). PGE2 increases lentiviral vector transduction efficiency of human HSC. Mol. Ther. *24* (S1), 229, (abstract).

Kallinikou, K., Anjos-Afonso, F., Blundell, M.P., Ings, S.J., Watts, M.J., Thrasher, A.J., Linch, D.C., Bonnet, D., and Yong, K.L. (2012). Engraftment defect of cytokine-cultured adult human mobilized CD34+ cells is related to reduced adhesion to bone marrow niche elements. Br. J. Haematol. *158*, 778–787.

Kerre, T.C., De Smet, G., De Smedt, M., Offner, F., De Bosscher, J., Plum, J., and Vandekerckhove, B. (2001). Both CD34+38+ and CD34+38− cells home specifically to the bone marrow of NOD/LtSZ scid/scid mice but show different kinetics in expansion. J. Immunol. *167*, 3692–3698.

Kiernan, J., Damien, P., Monaghan, M., Shorr, R., McIntyre, L., Fergusson, D., Tinmouth, A., and Allan, D. (2016). Clinical studies of ex vivo expansion to accelerate engraftment after umbilical cord blood transplantation: a systematic review. Transfus. Med. Rev. http://dx.doi.org/10.1016/j.tmrv.2016.12.004.

Larochelle, A., Gillette, J.M., Desmond, R., Ichwan, B., Cantilena, A., Cerf, A., Barrett, A.J., Wayne, A.S., Lippincott-Schwartz, J., and Dunbar, C.E. (2012). Bone marrow homing and engraftment of human hematopoietic stem and progenitor cells is mediated by a polarized membrane domain. Blood *119*, 1848–1855.

Lidonnici, M.R., Aprile, A., Frittoli, M.C., Mandelli, G., Paleari, Y., Spinelli, A., Gentner, B., Zambelli, M., Parisi, C., Bellio, L., et al. (2016). Plerixafor and G-CSF combination mobilizes hematopoietic stem and progenitors cells with a distinct transcriptional profile and a reduced in vivo homing capacity compared to Plerixafor alone. Haematologica http://dx.doi.org/10.3324/haematol.2016.154740.

Majeti, R., Park, C.Y., and Weissman, I.L. (2007). Identification of a hierarchy of multipotent hematopoietic progenitors in human cord blood. Cell Stem Cell *1*, 635–645.

Mazurier, F., Doedens, M., Gan, O.I., and Dick, J.E. (2003). Rapid myeloerythroid repopulation after intrafemoral transplantation of NOD-SCID mice reveals a new class of human stem cells. Nat. Med. *9*, 959–963.

McDermott, S.P., Eppert, K., Lechman, E.R., Doedens, M., and Dick, J.E. (2010). Comparison of human cord blood engraftment between immunocompromised mouse strains. Blood *116*, 193–200.

McKenzie, J.L., Gan, O.I., Doedens, M., and Dick, J.E. (2007). Reversible cell surface expression of CD38 on CD34-positive human hematopoietic repopulating cells. Exp. Hematol. *35*, 1429–1436.

Michallet, M., Philip, T., Philip, I., Godinot, H., Sebban, C., Salles, G., Thiebaut, A., Biron, P., Lopez, F., Mazars, P., et al. (2000). Transplantation with selected autologous peripheral blood CD34+Thy1+ hematopoietic stem cells (HSCs) in multiple myeloma: impact of HSC dose on engraftment, safety, and immune reconstitution. Exp. Hematol. *28*, 858–870.

Miller, P.H., Knapp, D.J.H.F., Beer, P.A., MacAldaz, M., Rabu, G., Cheung, A.M.S., Wei, L., and Eaves, C.J. (2016). Early production of human neutrophils and platelets posttransplant is severely compromised by growth factor exposure. Exp. Hematol. *44*, 635–640.

Naldini, L. (2015). Gene therapy returns to centre stage. Nature *526*, 351–360.

Negrin, R.S., Atkinson, K., Leemhuis, T., Hanania, E., Juttner, C., Tierney, K., Hu, W.W., Johnston, L.J., Shizuru, J.A., Stockerl-Goldstein, K.E., et al. (2000). Transplantation of highly purified CD34+Thy-1+ hematopoietic stem cells in patients with metastatic breast cancer. Biol. Blood Marrow Transpl. *6*, 262–271.

Notta, F., Doulatov, S., Laurenti, E., Poeppl, A., Jurisica, I., and Dick, J.E. (2011). Isolation of single human hematopoietic stem cells capable of long-term multilineage engraftment. Science *333*, 218–221.

Palchaudhuri, R., Saez, B., Hoggatt, J., Schajnovitz, A., Sykes, D., Tate, T., Czechowicz, A., Kfoury, Y., Ruchika, F., Rossi, D., et al. (2016). Non-genotoxic conditioning for hematopoietic stem cell transplantation using a hematopoietic-cell-specific internalizing immunotoxin. Nat. Biotechnol. *34*, 738–747.

Petrillo, C., Cesana, D., Piras, F., Bartolaccini, S., Naldini, L., Montini, E., and Kajaste-Rudnitski, A. (2015). Cyclosporin a and rapamycin relieve distinct lentiviral restriction blocks in hematopoietic stem and progenitor cells. Mol. Ther. *23*, 352–362.

Sessa, M., Lorioli, L., Fumagalli, F., Acquati, S., Redaelli, D., Baldoli, C., Canale, S., Lopez, I.D., Morena, F., Calabria, A., et al. (2016). Lentiviral haemopoietic stem-cell gene therapy in early-onset metachromatic leukodystrophy: an ad-hoc analysis of a non-randomised, open-label, phase 1/2 trial. Lancet *388*, 476–487.

Stein, S., Ott, M.G., Schultze-Strasser, S., Jauch, A., Burwinkel, B., Kinner, A., Schmidt, M., Krämer, A., Schwäble, J., Glimm, H., et al. (2010). Genomic instability and myelodysplasia with monosomy 7 consequent to EVI1 activation after gene therapy for chronic granulomatous disease. Nat. Med. *16*, 198–204.

Wang, C.X., Sather, B.D., Wang, X., Adair, J., Khan, I., Singh, S., Lang, S., Adams, A., Curinga, G., Kiem, H.P., et al. (2014). Rapamycin relieves lentiviral vector transduction resistance in human and mouse hematopoietic stem cells. Blood *124*, 913–923.

Stem Cell Reports, Volume *8*

Supplemental Information

Efficient Ex Vivo Engineering and Expansion of Highly Purified Human Hematopoietic Stem and Progenitor Cell Populations for Gene Therapy

Erika Zonari, Giacomo Desantis, Carolina Petrillo, Francesco E. Boccalatte, Maria Rosa Lidonnici, Anna Kajaste-Rudnitski, Alessandro Aiuti, Giuliana Ferrari, Luigi Naldini, and Bernhard Gentner

Figure S1

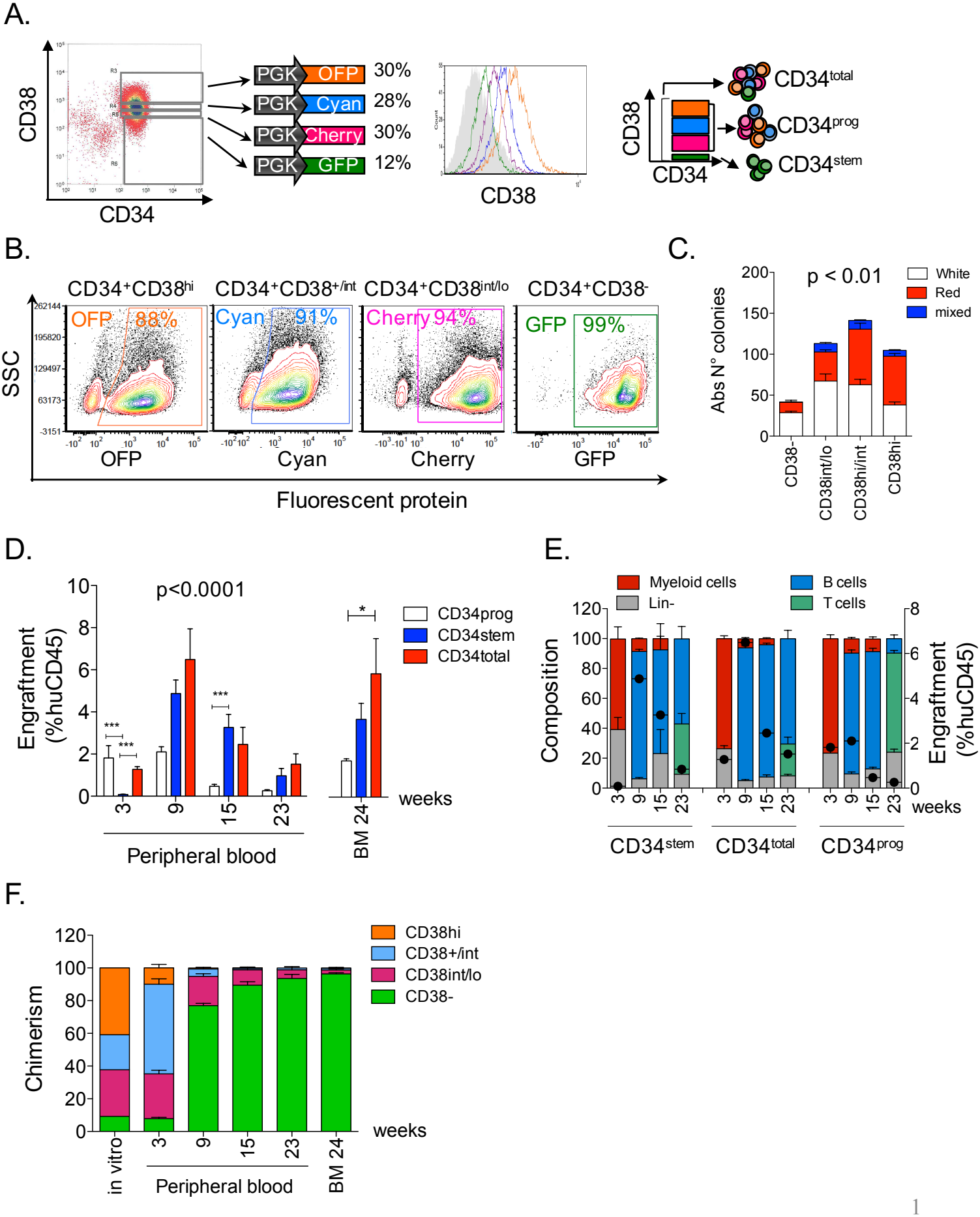
A.
CD38
CD34
PGK OFP 30%
PGK Cyan 28%
PGK Cherry 30%
PGK GFP 12%
CD38
CD34total
CD34prog
CD34stem
CD34
B.
CD34+CD38hi
CD34+CD38+/int
CD34+CD38int/lo
CD34+CD38-
OFP 88%
Cyan 91%
Cherry 94%
GFP 99%
SSC
OFP
Cyan
Cherry
GFP
Fluorescent protein
C.
p < 0.01
White
Red
mixed
Abs N° colonies
CD38-
CD38int/lo
CD38hi/int
CD38hi
D.
p<0.0001
Engraftment (%huCD45)
CD34prog
CD34stem
CD34total
weeks
Peripheral blood
BM 24
E.
Myeloid cells
Lin-
B cells
T cells
Composition
Engraftment (%huCD45)
weeks
CD34stem
CD34total
CD34prog
F.
Chimerism
CD38hi
CD38+/int
CD38int/lo
CD38-
weeks
in vitro
Peripheral blood
BM 24

Figure S1. In vivo tracking of hematopoietic reconstitution by $CD34^+$ mPB subpopulations. Replicate experiment, related to Figure 1.

A. Representative sorting gates applied to mPB $CD34^+$ cells. Four subpopulations differing in CD38 expression levels were randomly assigned to transduction with LVs expressing 1 of 4 fluorescent proteins (PGK: phosphoglycerate kinase promoter; OFP: orange fluorescent protein; Cyan: cyan/blue fluorescent protein; Cherry: red fluorescent protein; GFP: enhanced green fluorescent protein). Subpopulation frequency within total $CD34^+$ cells and CD38 expression upon post-sorting re-analysis are shown (histogram plot). The scheme on the right shows the subpopulations transplanted into sub-lethally irradiated NSG mice, together with the nomenclature applied to the 3 groups. When different subpopulations were mixed, their relative frequency during sorting was maintained.

B. Representative transduction efficiency of the different subpopulations ($CD34^+CD38^{hi}$, $CD34^+CD38^{+/int}$, $CD34^+CD38^{int/lo}$, $CD34^+CD38^-$), as measured in the myeloid colonies after 14 days of culture.

C. In vitro clonogenic potential assessed by the CFC assay performed on the transduced cells (1000 cells/plate) – the total number (mean ± SEM) of different types of colonies (white, red and mixed) was counted for the different subpopulations (n=4 dishes). Data were analyzed by One-way analysis of variance (ANOVA) for red, white and mixed colonies. Bonferroni's Multiple Comparison Test (* $p<0.05$, ** $p<0.01$, *** $p<0.001$) for white colonies: $CD38^-$ vs $CD38^{int/lo}$ **, $CD38^-$ vs $CD38^{int/hi}$ **; for red colonies: $CD38^-$ vs $CD38^{int/lo}$ *, $CD38^-$ vs $CD38^{int/hi}$ ***, $CD38^-$ vs $CD38^{hi}$ ***; for mixed colonies: $CD38^-$ vs $CD38^{int/lo}$ ***, $CD38^-$ vs $CD38^{int/hi}$ ***, $CD38^-$ vs $CD38^{hi}$ **.

D. Human $CD45^+$ cell engraftment (mean ± SEM) in peripheral blood and bone marrow of NSG mice at the indicated time point (weeks post-transplant). $CD34^{total}$: n=6 mice; $CD34^{prog.}$: n=7 mice; $CD34^{stem}$: n=6 mice. Data were analyzed by Two-way analysis of variance (ANOVA) after log transformation. Significance values from Bonferroni's Multiple Comparison Test with respect to the $CD34^{stem}$ group are shown in the graph (* $p<0.05$, ** $p<0.01$, *** $p<0.001$).

E. Lineage composition (mean ± SEM; left axis) of the human $CD45^+$ cell graft (black dot; right axis) in the PB at the indicated n. of weeks post-transplantation of the different groups of mice. B cells, $CD19^+$; Myeloid cells, $CD13^+$, T cells, $CD3^+$; negative, lineage negative ($CD19^-$, $CD13^-$, $CD3^-$) cells.

F. Distribution of the 4 fluorescent proteins in the $CD34^{total}$ group before injection (in vitro) or within human $CD45^+$ cells sampled from the PB and BM at the indicated n. of weeks post-transplantation allows backtracking the origin of hematopoietic reconstitution to the originally transplanted cell subpopulations indicated in the legend.

Figure S2

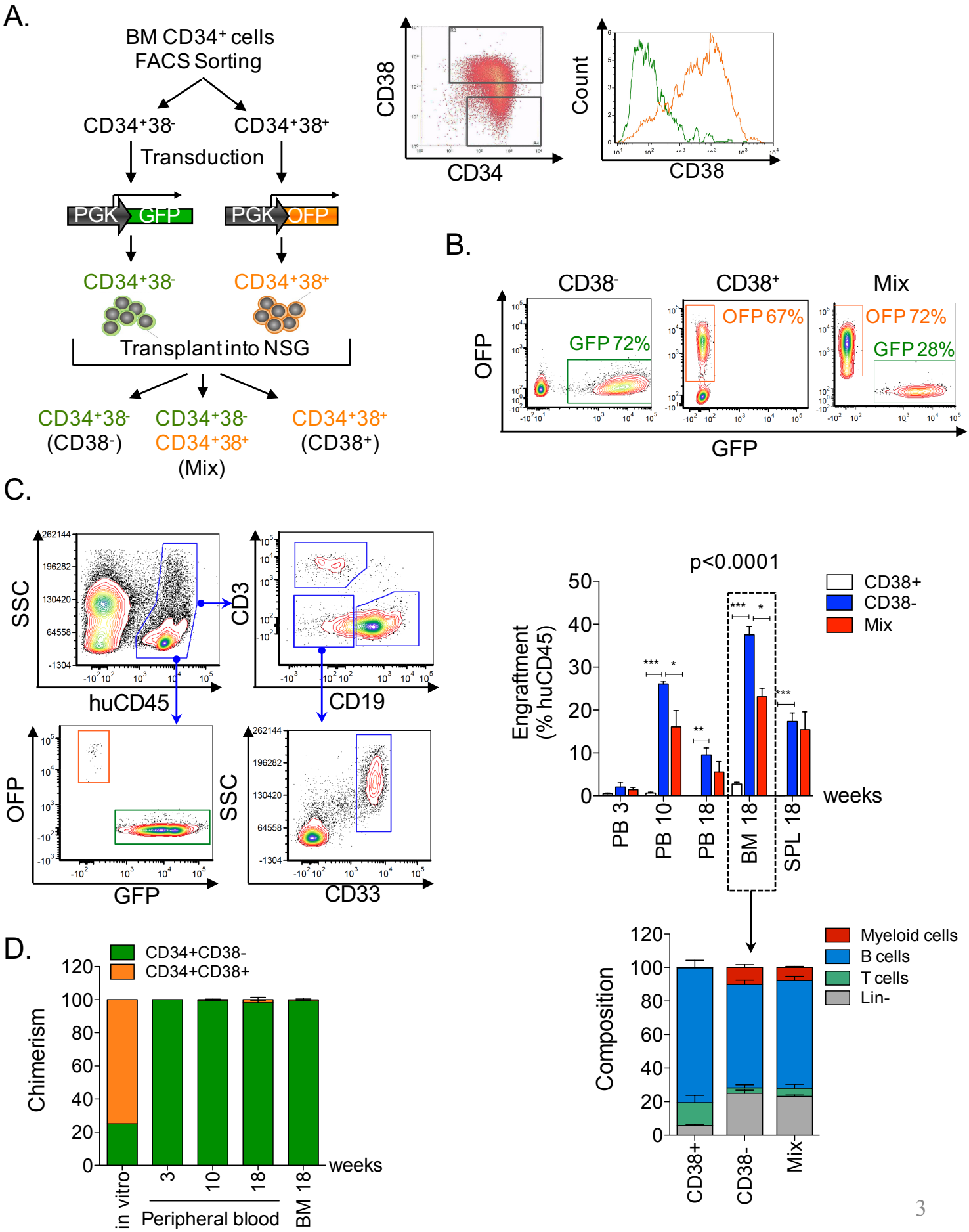
A.
BM CD34+ cells
FACS Sorting
CD34+38-
CD34+38+
Transduction
PGK GFP
PGK OFP
CD34+38-
CD34+38+
Transplant into NSG
CD34+38-
(CD38-)
CD34+38-
CD34+38+
(Mix)
CD34+38+
(CD38+)
CD38
CD34
Count
CD38
B.
CD38-
CD38+
Mix
OFP
GFP 72%
OFP 67%
OFP 72%
GFP 28%
GFP
C.
SSC
huCD45
CD3
CD19
OFP
GFP
SSC
CD33
p<0.0001
CD38+
CD38-
Mix
Engraftment
(% huCD45)
PB 3
PB 10
PB 18
BM 18
SPL 18
weeks
Composition
Myeloid cells
B cells
T cells
Lin-
CD38+
CD38-
Mix
D.
CD34+CD38-
CD34+CD38+
Chimerism
in vitro
3
10
18
BM 18
Peripheral blood
weeks

Figure S2. In vivo tracking of hematopoietic reconstitution by $CD34^+$ BM subpopulations. Related to Figure 1.

A. Experimental design and representative sorting gates applied to BM $CD34^+$ cells. $CD34^+CD38^+$ and $CD34^+CD38^-$ cells were transduced respectively with LV expressing OFP or GFP under the control of a PGK promoter. CD38 expression within transduced cells upon sorting is shown. The scheme on the left shown the subpopulations transplanted into sub-lethally irradiated NSG mice, together with the nomenclature applied to the 3 groups ($CD38^-$, n=3; $CD38^+$, n=3, Mix, n=3). When different subpopulations were mixed, their relative frequency during sorting was maintained.

B. Representative transduction efficiency of the different subpopulations ($CD38^-$, $CD38^+$ and Mix), as measured in the myeloid progeny after 2 days of culture.

C. Left panel: representative cytofluorimetric FACS plot to identify human $CD45^+$ cells in PB of NSG transplanted mice and the different lineages populations within $CD45^+$. Right panel: human $CD45^+$ cell engraftment (mean ± SEM) in PB, BM and spleen (SPL) of NSG mice at the indicated time point (weeks post-transplant). Lineage composition (mean ± SEM) of the human $CD45^+$ cell graft in the BM 18 weeks post-transplantation. B cells, $CD19^+$; Myeloid cells, $CD13^+$, T cells, $CD3^+$; negative, lineage negative ($CD19^-$, $CD13^-$, $CD3^-$) cells. Data were analyzed by Two-way analysis of variance (ANOVA) after log transformation. Significance values from Bonferroni's Multiple Comparison Test with respect to the $CD34^{stem}$ group are shown in the graph (* $p<0.05$, ** $p<0.01$, *** $p<0.001$).

D. Distribution of the 2 fluorescent proteins in the Mix group before injection (in vitro) or within human $CD45^+$ cells sampled from the PB and BM at the indicated n. of weeks post-transplantation allows back-tracing the origin of hematopoietic reconstitution to the originally transplanted cell subpopulations indicated in the legend.

Figure S3

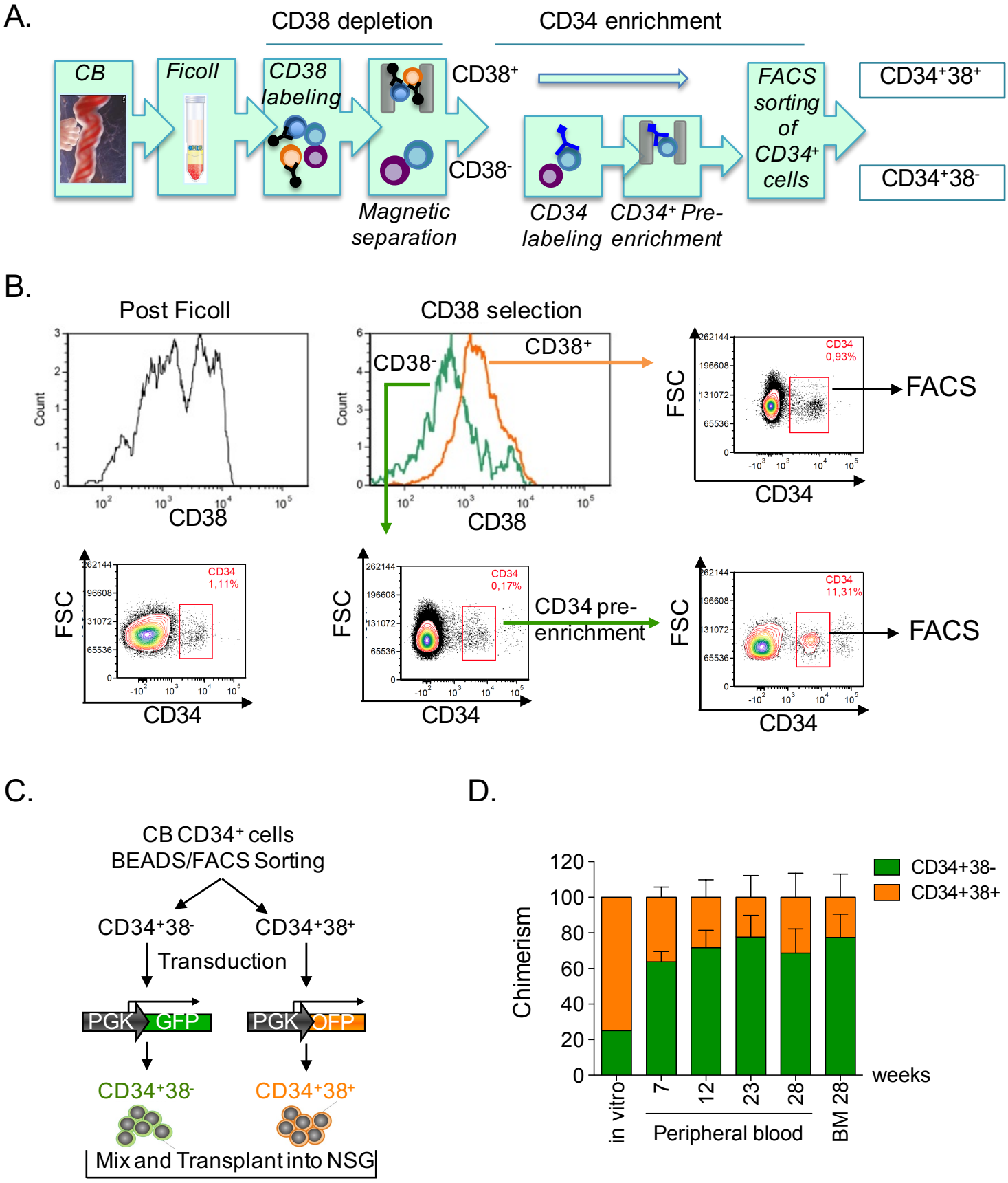
A.
CD38 depletion
CD34 enrichment
CB
Ficoll
CD38 labeling
CD38+
CD38-
Magnetic separation
CD34 labeling
CD34+ Pre-enrichment
FACS sorting of CD34+ cells
CD34+38+
CD34+38-
B.
Post Ficoll
CD38 selection
Count
CD38
CD38-
CD38+
FSC
CD34
CD34 0,93%
FACS
CD34 1,11%
CD34 0,17%
CD34 pre-enrichment
CD34 11,31%
C.
CB CD34+ cells
BEADS/FACS Sorting
CD34+38-
CD34+38+
Transduction
PGK GFP
PGK OFP
Mix and Transplant into NSG
D.
Chimerism
CD34+38-
CD34+38+
in vitro
7
12
23
28
BM 28
Peripheral blood
weeks

Figure S3. In vivo tracking of hematopoietic reconstitution by $CD34^+$ CB subpopulations sorted by a bead-based procedure. Related to Figure 1.

A. Schematic representation of the beads-based sorting procedure applied to separate $CD38^+$ and $CD38^-$ cells from CB.

B. Representative FACS plots showing the percentage of $CD34^+$ cells during the different steps of bead-based selection procedure (post-Ficoll, CD38 selection, CD34 sorting).

C. Experimental design applied to CB $CD34^+$ cells. $CD34^+CD38^+$ and $CD34^+CD38^-$ sorted cells were transduced respectively with LV expressing OFP or GFP under the control of a PGK promoter. The two subpopulations were mixed in a naturally ratio and transplanted into sub-lethally irradiated NSG mice (n=3).

D. Distribution of the 2 fluorescent proteins in the Mix group before injection (in vitro) or within human $CD45^+$ cells sampled from the PB and BM at the indicated n. of weeks post-transplantation allows back-tracing the origin of hematopoietic reconstitution to the originally transplanted cell subpopulations indicated in the legend.

Figure S4

A.

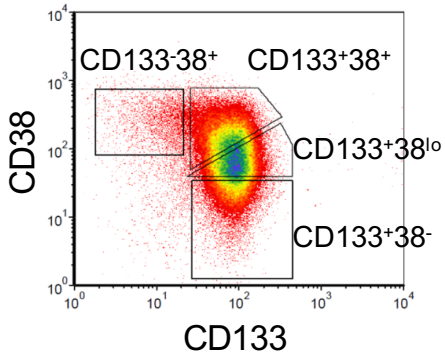

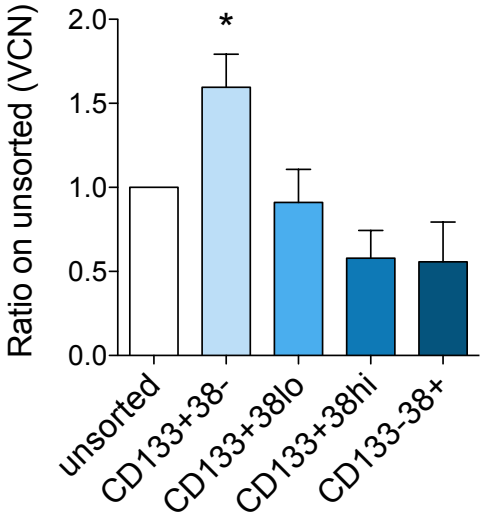

B.

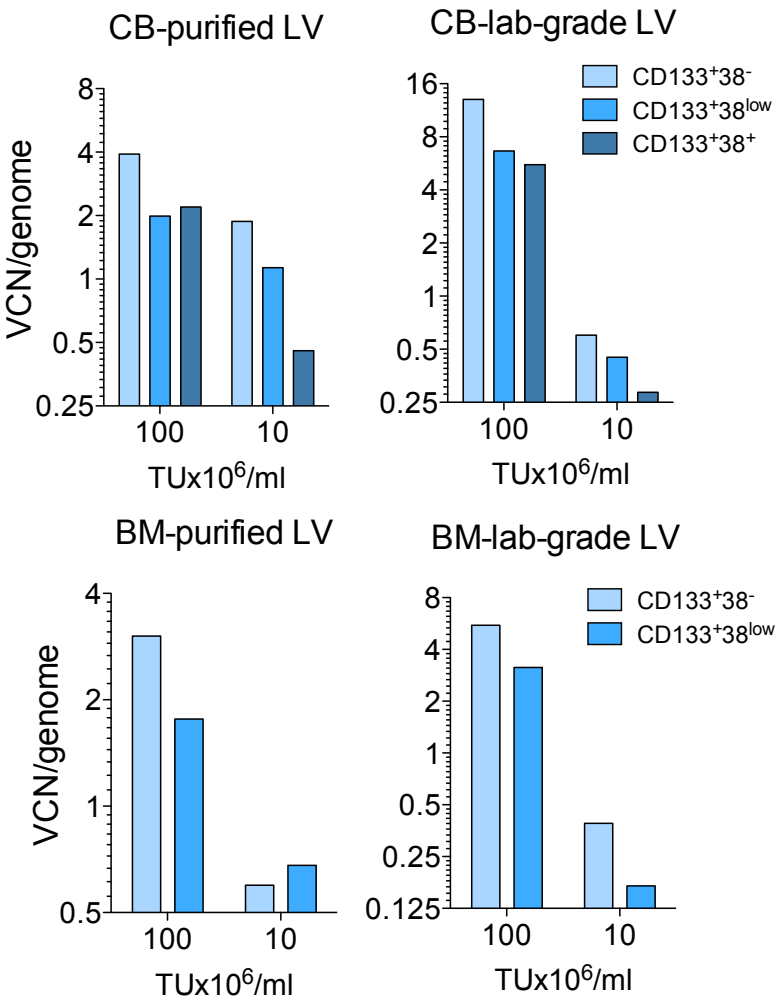

C.

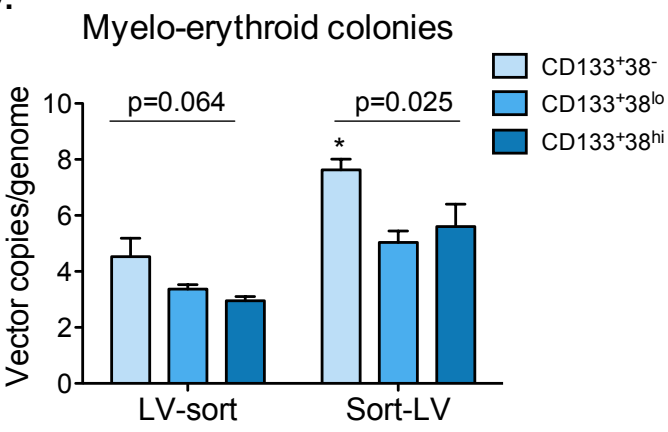

D.

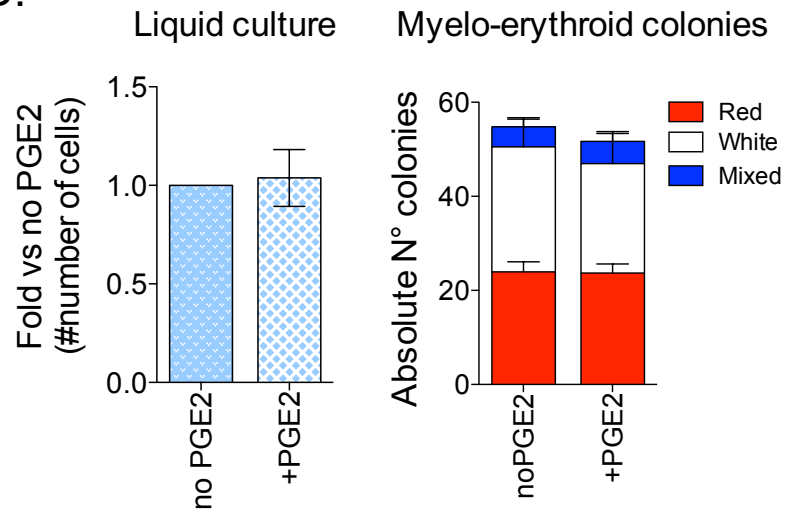

E.

Protocol of Transduction	Hits	VCN
38h	1	0.81
24h +PGE$_2$	1	3.5
38h +PGE$_2$	1	2.25

Protocol of Transduction	Hits	VCN
24h	1	0.45
38h	1	0.34
24h +PGE$_2$	1	0.98
38h +PGE$_2$	1	0.83

Figure S4. Increased transduction of HSPC by lentiviral vectors. Related to Figure 3.

A. Human cord blood-derived $CD34^+$ cells were FACS-sorted according to CD133 and CD38 expression as shown. The sorted subpopulations were transduced with LV-GFP and transduction efficiency was measured. Quantitative Real-Time PCR (qPCR) analysis of DNA extracted after 2 weeks in culture was used to determine vector copy number (VCN). Results obtained from 3 independent CB donors using 4 different LVs. Data were analyzed by Wilcoxon signed-rank test (*$p<0.05$).

B. Human CB or BM $CD34^+$ cells were FACS-sorted as described in panel A. Sorted populations were transduced with lab-grade or GMP-grade, purified LV at different TU/ml and transduction efficiency was measured by determining the VCN by qPCR. $100x10^6$ TU/ml corresponds to an moi of 100, while $10x10^6$ TU/ml corresponds to an moi of 10.

C. In order to test whether this increased permissiveness of $CD38^-$ cells towards LV transduction is a cell-intrinsic property of more primitive HSPC or due to external factors such as cell competition for vector particles, we wondered whether the CD38- subset is also more targeted by LV when transducing bulk $CD34^+$ cultures. We thus made a side-by-side comparison of two protocols: in the first protocol, cells are sorted first, and purified populations are exposed to the LV (protocol named "sort-LV"); in the second protocol, bulk $CD34^+$ cells are LV-transduced, and CD38 subpopulations are sorted 24hr later and cultured separately in order to assess transduction levels in the purified populations (protocol named "LV-sort"). Importantly, pre-stimulation times before and cell density at the moment of LV exposure were kept constant in both protocols to minimize any potential bias impacting on transducibility. VCN measured in the colony outgrowth after 14 days in methylcellulose is shown for 3 independent CB donors transduced with LV-GFP at 10^8 TU/ml. For each group (LV-sort or Sort-LV) data were analyzed by One-way analysis of variance (ANOVA). *, $p<0.05$ with respect to $CD38^{low}$ cells by Bonferroni's Multiple Comparison Test.

D. Left plot: Ex vivo proliferation of mPB-derived HSPC transduced in the presence of $dmPGE_2$ relative to the respective control group transduced without PGE_2 (n=5 donors). Data were analyzed by Wilcoxon signed-rank test. Right plot: In vitro clonogenic potential assessed by CFC assay performed on $CD34^+$ mPB transduced with or without $dmPGE_2$. The total number (mean ± SEM) of different types of colonies (white, red and mixed) was counted for the 2 conditions (n=3 donors). Data were analyzed by One-way analysis of variance (ANOVA) for red, white and mixed colonies, and no statistically significant differences emerged.

E. Vector copy number (VCN) in the myeloid outgrowth of $CD34^+CD38^-$ cells (n=2 donors) transduced with GMP-grade beta-globin expressing lentiviral vector according to the indicated transduction protocol. These $CD34^+CD38^-$ cells were xenotransplanted (see Figure 3I-K).

Supplemental Experimental Procedures

Lentiviral vectors used in this study

Third generation self-inactivating (SIN) LV (PGK.GFP, PGK.OFP, PGK.Cyan, PGK.BFP, PGK.mCherry, SP146/gp91^{phox}P.gp91^{phox}±126T), integrase-defective LV (IDLV) and SIN-retroviral vector (SIN-RV) expressing GFP under the control of an internal PGK promoter stocks were prepared, concentrated and titered as previously described (Follenzi et al., 2000; Lombardo et al., 2007; Montini et al., 2006). SIN-LV P90A and N74D capsid mutants as well as Baboon (BaEV-LVs) and feline RD114-TR envelope pseudotyped LVs were produced as described (Girard-Gagnepain et al., 2014; Marin et al., 2016; Petrillo et al., 2015). GMP-grade LV (PGK.GFP or beta-globin expressing LV) was manufactured by MolMed.

HSPC culture, transduction and expansion protocols

HSPC pre-stimulation and transduction was performed in serum-free medium, at a cell density of 1x10^6 cells/ml. In case cells went into ex vivo expansion cultures, cell density was reduced to 1x10^5 cells/ml to avoid accumulation of paracrine factors jeopardizing HSC maintenance. Culture media and cytokines varied according to cell source and application, in order to be in line with our standards validated over the years.

Cord blood HSPC was cultured in StemSpan medium (Stem Cell Technologies) containing the following cocktail of cytokines: 20 ng/ml IL-6, 50 ng/ml TPO, 100 ng/ml SCF, and 100 ng/ml FLT-3L (all from Peprotech). During ex vivo expansion (±SR1), cytokine concentrations were adapted to the ones used in pertinent publications (Boitano et al., 2010).

Bone marrow and mobilized peripheral blood HSPC were cultured, as in our clinical trials, in CellGro medium (Cell Genix) containing the following cocktail of cytokines: 60 ng/ml IL-3, 100 ng/ml TPO, 300 ng/ml SCF, and 300 ng/ml FLT-3L (all from Cell Genix). As indicated in the text, IL-3 was removed from the updated transduction protocol of CD34$^+$CD38$^-$ mPB cells (Figures 2F-G, 3I-K, 4), without any notable differences in transduction efficiency. Expansion of mPB CD34$^+$CD38$^-$ cells (cell density: 10^5 cells/ml) was carried out in StemMacs human HSC expansion medium (Miltenyi) using the following cytokines: 100ng/ml SCF, 100ng/ml FLT3L, 50ng/ml TPO, 50ng/ml IL-6 ± UM171 ± SR1.

LV transduction protocols were as follows:

Short protocol name	Applied to	Pre-stimulation	First round of LV transduction	Recovery	Second round of LV transduction
60-62hr/2 Hit	clinical standard	22±2 hr	14±2 hr	10±2 hr	14±2 hr
46-48hr/1 Hit	CB, BM, mPB unless otherwise indicated	22±2 hr	24±2 hr	-	-
36-38hr/1Hit	mPB	22±2 hr	14±2 hr	-	-
24hr/1Hit	mPB	14±1 hr	10±1 hr	-	-

A round of LV transduction consisted in adding 10^8 transducing units/ml (multiplicity of infection: 100, unless otherwise indicated) to the cell cultures. Wells were pre-coated with RetroNectin (Takara) in experiments performed with purified LVs.

Prostaglandin E_2

16,16-dimethyl Prostaglandin E_2 ($dmPGE_2$), formulated in methyl acetate solution, was purchased from Cayman Chemical. Upon arrival, the solvent was evaporated using a Speed Vac system, resuspended in DMSO at a 10mM concentration (1000x), aliquoted and cryopreserved at -80°C for no longer than 12 months. Upon use, the required number of 1000x $dmPGE_2$ aliquots were thawed on ice, pre-diluted in culture medium and added to the HSPC culture (10µM final concentration), either at the beginning of culture or 120 minutes before LV transduction. Cells were washed no earlier than 14 hours after adding the LV.

In vitro readouts

Myeloid differentiation liquid cultures were carried out in IMDM medium containing 10% FBS and early acting cytokines such as SCF and IL-3).

Clonogenic assays were plated at the end of LV transduction. Cells were washed, counted and resuspended in complete human Methocult medium (Stem Cell Technologies) at a concentration of 800-1000 cells/ml. Fifteen days later, colonies were scored by light microscopy for number and morphology. CFU-E and BFU-E were scored as erythroid colonies, while CFU-G, CFU-M and CFU-GM as myeloid and CFU-GEMM as mixed colonies. Human differentiated cells from CFC were harvested from a single plate (pool of colonies) and mixed into a single cell suspension. Cells were washed and resuspended in PBS containing 2% FBS. For immunostaining, cells were incubated with anti-human receptor blocking antibodies for 15 min at 4 °C and stained for 20 min at 4 °C with anti-human CD235a and CD33 antibodies (for antibodies see Table S1). To exclude dead cells from the analysis, cells were washed and resuspended in PBS containing 10 ng/ml 7-aminoactinomycin D (7-AAD).

Peripheral blood analysis

Mice were bled via the tail vein following analgesia. For each mouse, 250µl of peripheral blood was added to 10µL of PBS containing 45mg/mL EDTA. For immunostaining a known volume of whole blood (100µl) was incubated with anti-human Fc receptor blocking antibodies for 10 min at room temperature then incubated in the presence of monoclonal antibodies (for a list of antibodies, see Table S1) for 15 min at room temperature. Erythrocytes were removed by lysis with the TQ-Prep workstation (Beckman-Coulter) in the presence of an equal volume of FBS (100µl).

Bone marrow analysis

BM aspirates were obtained under deep anesthesia, by inserting a 26G needle into the distal femur shaft and aspirating the content into a 1ml syringe containing 100-200µl PBS. At the experimental endpoint, mice were humanely euthanized, and BM cells were obtained by flushing the femurs in PBS 2% FBS solution. Cells ($1x10^6$ cells) were washed, resuspended in 100µl of PBS containing 2% FBS, and incubated with anti-human and/or anti-mouse FcγIII/II receptor (Cd16/Cd32) blocking antibodies for 15 min at 4°C. Staining was performed with monoclonal antibodies (Table S1) for 20 min at 4°C.

Spleen analysis

Spleens were dissociated into single-cell suspensions, passed through 40µm nylon filter, and washed in cold phosphate buffered saline (PBS) containing 2mM EDTA

and 0.5% bovine serum albumine (BSA). Cells were incubated with anti-mouse FcγIII/II receptor (Cd16/Cd32) blocking antibodies for 15 min at 4°C and stained with anti-mouse monoclonal antibodies (Table S1) for 20 min at 4°C. To exclude dead cells from the analysis, cells were washed and resuspended in PBS containing 10ng/ml 7-aminoactinomycin D (7-AAD).

Quantitative PCR

Genomic (g)DNA was extracted using QIAmp DNA micro kit (Qiagen) or QIAmp DNA mini kit according to the starting number of cells (as suggested by manufacturer). DNA was quantified and assessed for purity. Vector copies per diploid genome (vector copy number, VCN) of the integrated lentiviral vectors were quantified by quantitative TaqMan PCR (qPCR) starting from 10-100 ng of template gDNA using the following primers (HIV sense: 5'-TACTGACGCTCTCGCACC-3'; HIV antisense: 5'-TCTCGACGCAGGACTCG-3') and probe (FAM 5'-ATCTCTCTCCTTCTAGCCTC-3') against the primer binding site region of LVs. Analysis was performed no earlier than 7-14 days post-transduction, to give enough time for non-integrated genomes to disappear during cell division. Endogenous DNA amount was quantified by a primer/probe set against the human telomerase gene (Telo sense: 5'-GGCACACGTGGCTTTTCG-3'; Telo antisense: 5'-GGTGAACCTCGTAAGTTTATGCAA-3'; Telo probe: VIC 5'-TCAGGACGTCGAGTGGACACGGTG-3' TAMRA). Copies per genome were calculated by the formula = [ng LV/ng endogenous DNA] - [number of LV integrations in the standard curve]. The standard curve for qPCR was generated by using the CEMA301 cell line stably carrying four vector integrants, which were previously determined by Southern blot analysis. All reactions were carried out in duplicate or triplicate on an Viia7 Real time PCR system (Applied Biosystems). As an alternative, VCN was determined by digital droplet PCR (ddPCR) on a QX200 Droplet Digital PCR System (Biorad).

Transduction efficiency by vector variants and quantification of replication intermediates was assessed by the following molecular analyses: IDLV: quantification of total lentiviral DNA (integrated and non-integrated) was performed as previously described (Mátrai et al., 2011), at three days post-transduction. Copy number of the reverse transcribed retroviral vector genome (both integrated and non-integrated) was performed by quantitative droplet digital PCR (ddPCR) discriminating it from plasmid carried over from the transient transfection using the following primers: RT-RV; ΔU3 sense: 5'-CGAGCTCAATAAAAGAGCCCAC-3', U3 antisense: 5'-GAGTCCTGCGTCGGAGAGAG-3'. For DNA replication intermediates analysis, cells were lysed and processed 6 and 24 hours post-transduction in Monini lysis buffer as previously described (Petrillo et al., 2015) followed by ddPCR. Primers and probes used to quantify late-RT and 2LTR replication intermediates were described (Petrillo et al., 2015).

Table S1. List of anti-human antibodies used for flow cytometry.

Antibody	Fluorochrome	Clone	Company	Code
hCD45	APC-eFluor780	HI30	eBioscience	47-0459-42
hCD45	PercP Cy5.5	H130	BioLegend	304028
hCD19	PE-Cy7	HIB19	BioLegend	302216
hCD3	PE	SK7	BD	345765
hCD3	PB	UCHT1	BioLegend	300431
hCD13	APC	WM15	BD	557454
hCD33	APC	AC104.3E3	Miltenyi Biotec	130-091-731
hCD33	PE-Cy7	P67.6	BD	333952
hCD235a	APC	REA175	Miltenyi Biotec	130-100-270
hCD34	VioBlue	AC136	Miltenyi Biotec	130-095-393
hCD38	PE-Vio770	IB6	Miltenyi Biotec	130-099-151
hCD90	APC	5E10	BD Bioscience	559869
hCD45RA	PE	T6D11	Miltenyi Biotec	130-092-248
hCD133	PE	293C3	Miltenyi Biotec	130-090-853
FcR Blocking Reagent			Miltenyi Biotec	130-059-901

Supplemental References:

Follenzi, A., Ailles, L.E., Bakovic, S., Geuna, M., Naldini, L., 2000. Gene transfer by lentiviral vectors is limited by nuclear translocation and rescued by HIV-1 pol sequences. Nat Genet 25, 217–222.

Girard-Gagnepain, A., Amirache, F., Costa, C., Levy, C., Frecha, C., Fusil, F., Nègre, D., Lavillette, D., Cosset, F.L., Verhoeyen, E., 2014. Baboon envelope pseudotyped LVs outperform VSV-G-LVs for gene transfer into early-cytokine-stimulated and resting HSCs. Blood 124, 1221–1231.

Lombardo, A., Genovese, P., Beausejour, C.M., Colleoni, S., Lee, Y.-L., Kim, K. a, Ando, D., Urnov, F.D., Galli, C., Gregory, P.D., Holmes, M.C., Naldini, L., 2007. Gene editing in human stem cells using zinc finger nucleases and integrase-defective lentiviral vector delivery. Nat. Biotechnol. 25, 1298–1306.

Marin, V., Stornaiuolo, A., Piovan, C., Corna, S., Bossi, S., Pema, M., Giuliani, E., Scavullo, C., Zucchelli, E., Bordignon, C., Rizzardi, G.P., Bovolenta, C., 2016. RD-MolPack technology for the constitutive production of self-inactivating lentiviral vectors pseudotyped with the nontoxic RD114-TR envelope. Mol. Ther. Methods Clin. Dev. 3, 16033.

Mátrai, J., Cantore, A., Bartholomae, C.C., Annoni, A., Wang, W., Acosta-Sanchez, A., Samara-Kuko, E., De Waele, L., Ma, L., Genovese, P., Damo, M., Arens, A., Goudy, K., Nichols, T.C., von Kalle, C., Marinee, M.K., Roncarolo, M.G., Schmidt, M., Vandendriessche, T., Naldini, L., 2011. Hepatocyte-targeted expression by integrase-defective lentiviral vectors induces antigen-specific tolerance in mice with low genotoxic risk. Hepatology 53, 1696–1707.

Montini, E., Cesana, D., Schmidt, M., Sanvito, F., Ponzoni, M., Bartholomae, C., Sergi Sergi, L., Benedicenti, F., Ambrosi, A., Di Serio, C., Doglioni, C., von Kalle, C., Naldini, L., 2006. Hematopoietic stem cell gene transfer in a tumor-prone mouse model uncovers low genotoxicity of lentiviral vector integration. Nat Biotechnol 24, 687–696. doi:nbt1216 [pii]\r10.1038/nbt1216

Petrillo, C., Cesana, D., Piras, F., Bartolaccini, S., Naldini, L., Montini, E., Kajaste-Rudnitski, A., 2015. Cyclosporin A and Rapamycin Relieve Distinct Lentiviral Restriction Blocks in Hematopoietic Stem and Progenitor Cells. Mol. Ther. 23, 352–362.